R80-37

EFFECT OF WIND-MIXING ON THE THERMOCLINE FORMATION IN LAKES AND RESERVOIRS

by
Siegfried Bloss
and
Donald R.F. Harleman

Ralph M. Parsons Laboratory
for Water Resources and Hydrodynamics
Department of Civil Engineering
Massachusetts Institute of Technology
Cambridge, Massachusetts 02139

Report No. 249

Prepared with the support of the
Ford Professorship at MIT
and the
German Research Society

November 1979

MIT

DEPARTMENT
OF
CIVIL
ENGINEERING

SCHOOL OF ENGINEERING
MASSACHUSETTS INSTITUTE OF TECHNOLOGY
Cambridge, Massachusetts 02139

R80-37

EFFECT OF WIND-MIXING ON THE THERMOCLINE FORMATION IN LAKES AND RESERVOIRS

BY

Siegfried Bloss
and
Donald R. F. Harleman

Ralph M. Parsons Laboratory
for Water Resources and Hydrodynamics
Department of Civil Engineering
Massachusetts Institute of Technology
Cambridge, Massachusetts 02139

Report No. 249

Prepared with the support of the
Ford Professorship at MIT
and the
German Research Society

November 1979

ABSTRACT

This study is concerned with the effects of wind-induced turbulence on the seasonal development of the temperature structure in a lake or reservoir.

In an earlier version of the MIT Lake and Reservoir Model*, wind-induced entrainment at the thermocline was accounted for by an algorithm that equated the input of turbulent kinetic energy (TKE) by the wind and the increase of potential energy due to mixing across the thermocline. Based on recent publications on the parameterization of the TKE-balance at a density interface, this algorithm was changed to account also for transient and dissipative effects on the turbulent entrainment process.

Different versions of the modified model were used to predict the seasonal stratification cycle in two lakes of different size and in a reservoir. The results suggest that during periods of weak stratification the entrainment process is limited by transient effects, i.e. by the storage of TKE in the growing epilimnion, while for strong stratification the wind-induced TKE is largely dissipated into the hypolimnion by internal waves. Only for intermediate stratification is the conversion process of TKE into potential energy, i.e. entrainment, effective. If the temperature structure is dominated by advection, as in a reservoir, wind effects may become negligible.

The sensitivity of the new model to various parameters was also investigated.

*"Vertical Heat Transport Mechanisms in Lakes and Reservoirs" by K.A. Hurley Octavio, G.H. Jirka and D.R.F. Harleman, R.M. Parsons Laboratory Technical Report No. 227, August 1977

Acknowledgements

This study was carried out during an appointment of Dr. Siegfried Bloss as visiting Engineer at the R.M. Parsons Laboratory. The financial support of this appointment by the German Research Society is gratefully acknowledged.

The data used for the verification of the mathematical model were provided by: Dr. D.W. Schindler of the Freshwater Institute, Canada (Lake 226NE), the Virginia Electric and Power Company (Lake Anna), and the Power Authority of the State of New York (Schoharie Reservoir). The authors appreciate the assistance and cooperation of these organizations. The assistance of Ms. Ming-pin Wang in preparing the numerical model for application to Lake 226NE is gratefully acknowledged.

Computational work was performed at the MIT Information Processing Center. The report was skillfully typed by Ms. Janice Allen and Mrs. Beth Quivey.

TABLE OF CONTENTS

I Introduction

1.1 Thermal Stratification in Lakes and Reservoirs

Cycles of thermal stratification and destratification can be observed in most natural or man-made bodies of water, such as lakes or reservoir impoundments, which are exposed to an environment with continuously changing meteorological conditions. Solar and atmospheric radiation that penetrate a lake and are absorbed at different depths tend to establish a stable temperature gradient, a process that is partially eroded by turbulent mixing due to through-flows and by heat loss and wind shear at the surface. During a period of prevailing heat input, i.e., in spring and summer, these counteracting processes lead to the development of a two-layered temperature structure in a lake. A warm, usually well mixed upper layer (epilimnion) overlays a cool, stagnant lower layer (hypolimnion) and it is separated from it by a strong temperature gradient (thermocline). When heat loss becomes predominant, i.e. during fall, the epilimnion cools and grows deeper, thereby, eroding the thermocline and the lake eventually returns to its initial isothermal condition. A typical vertical temperature profile and the processes involved in its development are shown in Fig. 1.1.

Although temperature is only one water quality parameter among others, such as concentration of oxygen, nutrients and biological species, it is of predominant importance. Its magnitude controls the rate of production or conversion of chemical or biological species, its gradient, or the density gradient associated with it, influences the flow patterns in a lake or reservoir and enhances or dampens the vertical turbulent transport processes. Accurate modelling of the vertical temperature structure, therefore, is not only of scientific interest but also is a prerequisite for any further attempt to describe other water quality parameters.

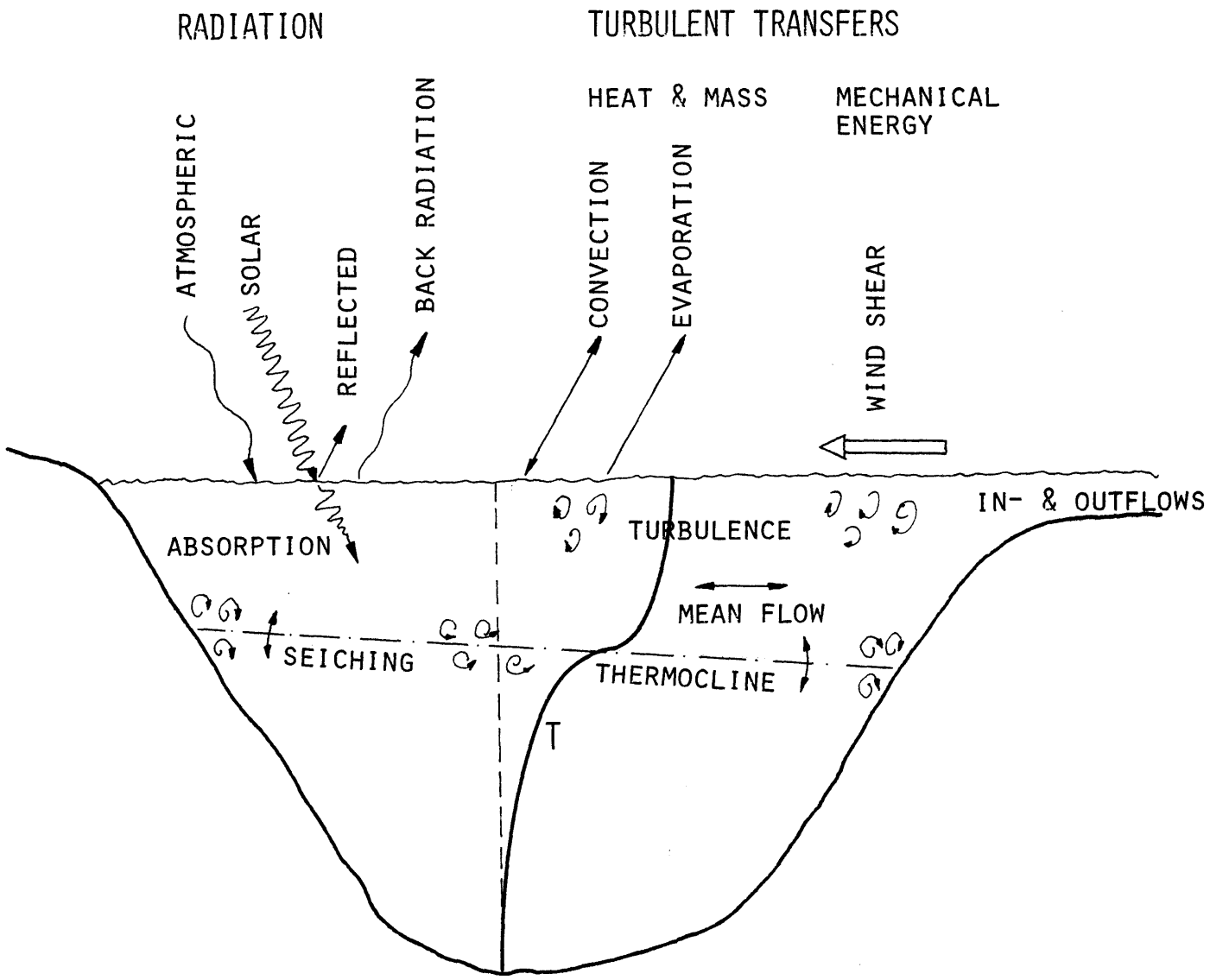

Figure 1-1 Transport Processes in a Lake and Across the Lake Surface

1.2 Limitations to the Development of a One-dimensional Temperature Structure

Measurements in lakes and reservoirs show that in most cases, isotherms are horizontal despite the multi-dimensional transfer and mixing processes, i.e. the temperature distribution is essentially one-dimensional in the vertical direction. However, large through-flows and/or strong winds acting on the surface may upset the one-dimensional structure.

In lakes and deep reservoirs with large residence times (defined as the ratio of their volume to the inflow rate) through-flows only affect a layer where their density matches the local density. However, in reservoirs where the residence time approaches the order of days, frequently termed "run-of-the-river" reservoirs, inflows may disturb the horizontal thermal structure by tilting the isotherms in the downstream direction. Orlob (1969) has proposed a densimetric Froude number as a measure for the presence of horizontal isotherms. In a modified form it can be defined as

$$Fr = \frac{u}{\sqrt{g'h}} = \left(\frac{LQ}{V}\right) \Big/ \sqrt{g \frac{\Delta\rho}{\rho_o} h} \qquad (1\text{-}1)$$

This Froude number relates the inertial forces due to throughflows (and represented by the mean horizontal velocity u) to the gravitational forces due the stratified structure. (L, h, V - length, mean depth, volume of a reservoir, Q = rate of throughflows, $\Delta\rho$ = density difference between epilimnion and hypolimnion, ρ_o = reference density, g = gravitational acceleration).

Based on experimental and theoretical work in stratified flow, Orlob gives a Froude number of the order of $1/\pi$ as a separating value between the horizontally stratified regime ($<<1/\pi$) and the vertically mixed regime ($>>1/\pi$). Since the quantities responsible for the formation of stratification (i.e. the short-wave solar radiation Φ_s and the absorption coefficient η)

are only vaguely represented in the above Froude number by $\Delta\rho$ (in Orlob's formulation by the mean density gradient) and, since the Froude number does not account for the locations of in- and outflows at all, the value given by Orlob can only be a rough estimate for the transition point between the two regimes. Measurements indicate that, at least for Froude numbers significantly less than unity, reservoirs exhibit horizontal isotherms.

Winds exert forces on lakes or reservoirs that tend to tilt the surface. As a result of this inclination, the thermocline in stratified lakes and reservoirs is then tilted in the opposite direction to a much greater extent. When the wind changes or stops, the surface and the thermocline start to oscillate but when the oscillations, called seiches, have died out after some time the body of water returns to its original one-dimensional thermal structure apart from some mixing due to currents associated with seiching. In the case of strong steady winds, the displacement of the thermocline may be so large that the hypolimnion is uncovered at one end of the lake or reservoir and, thus, the assumption of a one-dimensional system is no longer valid. An empirical formula given by Sverdrup (1945) relating the inclination of the surface to the wind speed and the mean water depth can be used to calculate the limiting wind speed W. If

$$W > 2 \cdot 10^3 \sqrt{d \cdot \frac{h}{L} \cdot \frac{\Delta\rho}{\rho}} \qquad (1\text{-}2)$$

a one-dimensional representation is no longer possible. (d = depth of epilimnion). Limiting wind speeds for average sized lakes in mid-latitude locations range in the order of 10m/s.

The scope of this work and the application of the models described in the following chapters are limited to lakes and reservoirs that satisfy

the criteria given above. If no temperature measurements are available to prove the validity of the assumption of a one-dimensional temperature structure, equations (1-1) and (1-2) can be used to support this assumption.

1.3 One-dimensional Lake and Reservoir Models

One-dimensional modelling of the temperature distribution in lakes or reservoirs requires an appropriate simplification or parameterization of all important multi-dimensional processes to fit into a one-dimensional scheme. Two types of models can be distinguished according to the approach they chose to achieve this goal.

Integral models average the effects of the various transport processes over horizontal layers of finite depth. The simplest version is a two-layer model, where the thickness and the temperature of the upper mixed layer are calculated from balances for the turbulent kinetic energy and for the internal energy, while the lower layer remains unaffected (Kraus and Turner (1967)). Denman (1973) improved the model of Kraus and Turner by including vertical advection and the absorption of short wave radiation in the lower layer. Tucker and Green (1977) further expanded this type of model to account for diffusion in the lower layer and for the effect of fetch on the surface transfer of wind energy. They applied this model on two lakes of different size and achieved good agreement with measurements, although the model does not account for the lake morphology. Since the above models were originally developed for temperature prediction in the upper ocean layer, they assume horizontal layers of infinite dimension rather than depth-dependent cross-sectional areas as given in a lake or reservoir.

Stefan and Ford (1975) were one of the first to develop an integral model for application to small lakes. Their variable area model includes the absorption of radiation in the hypolimnion but neglects diffusive transport. Unlike the previous models which solve the set of governing equations simultaneously, Stefan and Ford employed an alternating heating-mixing procedure. After a heating algorithm has been applied to calculate the local temperature change due to absorption of radiation and to surface heat transfer (including convective mixing in the case of surface heat loss), a wind-mixing algorithm takes account of the influence of wind on the formation of the thermocline. The model was applied to two lakes with good agreement.

Eddy diffusivity models attempt to incorporate the various effects of wind, horizontal flows and density gradients on the turbulent transport into a depth- and time-dependent eddy diffusivity. In the model of Munk and Anderson (1948) and in an expanded version by Sundaram and Rehm (1973), the turbulent exchange coefficient is expressed as the product of a neutral eddy diffusivity (determined by the surface wind shear and the current structure) and of a stability function (determined by a densimetric Richardson number). The model does not allow for depth-dependent absorption of solar radiation which is included in the surface boundary condition. The model yields reasonable values for the eddy diffusivity in weakly stratified lakes, but overpredicts it in the hypolimnion for strong stratification and underpredicts it in the upper epilimnion for high surface heat loss. For these situations, Sundaram and Rehm (1973) assume the minimum or maximum values, respectively, resulting from their relationship.

Spalding and Svensson (1976) compute turbulent exchange coefficients from a k, ε -turbulence model which solves the heat balance equation, the two horizontal momentum equations and the equations for the turbulent

kinetic energy (TKE), k, and for the dissipation of TKE, ε. Svensson (1978) applied the model to various stratified flow situations with very good results, but it remains questionable, whether long-term simulations of lake temperature cycles can be carried out with reasonable computer cost.

The MIT Lake and Reservoir model, which is described in the following chapter, takes advantage of both types of models. It solves the differential thermal energy equation for an accurate and detailed description of the transient vertical temperature profile, but avoids the difficulty of specifying a local eddy diffusivity by accounting for turbulent and convective mixing in separate integral routines.

1.4 Structure of the MIT Lake and Reservoir Model

The MIT Lake and Reservoir Model was designed to meet the basic requirements to be accomplished by a mathematical model, that is to be used as a predictive tool (Ryan and Harleman (1971); Hurley Octavio et.al. (1977)). It has to be able to:

a) describe the time-dependent temperature distribution with sufficient accuracy based on a minimal amount of input data,

b) investigate the sensitivity of the temperature distribution with respect to single parameters or processes

c) to predict the impact of natural or man-made changes on the temperature structure.

In order to simulate cycles of one or more years (requirements a) and c)) with a reasonable amount of computer time, the model should use a simple straightforward numerical scheme to solve the describing differential equation(s) with a time step of the order of one day. Sensitivity studies

can be carried out easier (requirement b,) if the model is structured. This allows investigation of the influence of single parameters independently of each other and the ability to improve the modelling of single processes on the basis of new research results without restructuring the whole model.

The MIT model, a one-dimensional, variable area model complies with these requirements as follows: It solves the governing differential equation using an explicit numerical scheme.

$$\frac{\partial T}{\partial t} + \frac{1}{A}\frac{\partial}{\partial z}(wAT) = \frac{E}{A}\frac{\partial}{\partial z}\left(A\frac{\partial T}{\partial z}\right) + \frac{q_i T_i - q_o T}{A} + \frac{\Phi_o(1-\beta)}{\rho c A}\frac{\partial}{\partial z}\left[Ae^{-\eta(z_s-z)}\right] \qquad (1\text{-}3a)$$

This equation relates the change of the vertical temperature profile $T(z,t)$ with time t to the heat fluxes due to vertical advection (vertical velocity w), to the vertical turbulent (or molecular) diffusion (eddy diffusivity E), to horizontal advection (in- and outflow per unit height q_i and q_o) and to absorption and transmission of solar radiation (global radiation flux at the surface Φ_o, short wave fraction transmitted through the surface $(1-\beta)$, extinction coefficient η). The origin of the vertical coordinate z is at the lake bottom, z_s is the elevation of the surface, A is the cross-sectional area of the lake, and ρ and c are density and specific heat. A vertical temperature distribution must be given as an initial condition,

$$T(z,0) = T_I(z) \qquad (1\text{-}3b)$$

As boundary conditions the heat flux at the surface is assumed to consist of the fluxes due to the convection (Φ_c), evaporation (Φ_e) and absorption ($\beta\Phi_o + \Phi_a$) and emission (Φ_b) of long wave radiation which are calculated from meteorological input data. The heat flux at the bottom is set equal to zero.

$$E\frac{\partial T}{\partial z} = \beta\Phi_o + \Phi_a - \Phi_c - \Phi_e - \Phi_b \qquad \text{at } z = z_s \tag{1-3c}$$

$$E\frac{\partial T}{\partial z} = 0 \qquad \text{at } z = 0 \tag{1-3d}$$

The vertical velocity w is calculated from the following mass balance

$$\frac{\partial (Aw)}{\partial z} = q_i - q_o \tag{1-4a}$$

with

$$w = 0 \qquad \text{at } z = 0 \tag{1-4b}$$

The distribution of q_i and q_o which also appear in the so-called external heat source term in eq. (1-3a) as a result of the incorporation of the two-dimensional horizontal flows into a one-dimensional vertical scheme, is calculated in separate subroutines. Outflow velocities are assumed to have a vertical Gaussian distribution around the actual outlet elevation. The height of the distribution is determined by the local density gradient. The distribution may be cut off by the surface (in the case of dam overflow or a surface outlet) or by the local bottom elevation (for a submerged outlet close to the bottom). Entrance mixing of inflows is accounted for by an entrainment factor, which specifies the additional flow entrained by a given inflow. The resulting mixed flow is assumed to spread with a Gaussian velocity distribution at a depth where the ambient density matches that of the mixed inflow. (See Ryan and Harleman, 1971.)

Equation (1-3a) does not account for vertical mixing due to surface heat loss and wind. Two mixing algorithms are therefore applied to the temperature profile calculated with eq. (1-3a) after each time step. Unstable density gradients (e.g. due to surface heat loss) are eliminated by mixing adjacent elements in a way that the internal energy of the resulting mixed layer is the same as that of the previous unstable profile.

Additional wind mixing is accounted for according to the rule that the rate of change of potential energy of a stratified water column due to mixing is equal to the rate of input of kinetic wind energy.

The above procedure avoids the necessity to specify a depth-dependent eddy diffusivity. The diffusion coefficient D is usually set equal to molecular diffusivity, but may be locally enhanced due to numerical dispersion.

1.5 Objectives of the Study

Having in mind the variety of processes that are involved in the formation of typical temperature profiles in a lake or a reservoir, it could be anticipated that different processes have similar effects on the temperature structure. For example, a low extinction coefficient allowing radiation to penetrate to greater depths may cause the same temperature rise at various depths as a high eddy diffusivity transporting heat downward by turbulent diffusion. On the other hand, the influence of these processes on the distribution of matter are quite different from each other. It is therefore necessary to model all processes as accurately as possible.

The effect of wind-induced entrainment across the thermocline was not well understood until recently when new experimental and theoretical research results on this topic became available. These results have been incorporated into the present MIT-model by means of a wind-mixing algorithm (Hurley Octavio et al. 1977). Taking into account wind-induced mixing as it was schematically described in the previous chapter the prediction quality of the MIT model improved in general, but the algorithm tended to overpredict the effect of wind-mixing during spring and fall periods.

The objective of this study is to correct this overprediction by including the following effects in the formulation of the wind-mixing algorithm:

a) transient effects of rapid growth of epilimnion depth during periods of weak stratification

b) dissipation effects during periods of strong stratification.

II Turbulent Entrainment Across a Density Interface

2.1 Description of Turbulent Entrainment Processes in Nature

Turbulent mixed layers often occur in nature which are agitated by a stirring mechanism on one boundary and are bounded by a density interface on the other side. Capping or underlying this interface is a layer of quiescent, often stably stratified fluid. The turbulent kinetic energy that is produced by the stirring agent, is transported into the central part of the layer where it is partially used to homogenize the fluid. At the interface, the remainder of this TKE, plus any that may be locally generated by shear, less that which is locally dissipated by viscosity or radiated into the quiescent fluid by internal waves, is transferred into potential energy by entraining quiescent fluid into the mixed layer. This entrainment (besides advective flows) finally determines the thickness of the mixed layer.

A typical example of a turbulent mixed layer is the atmospheric boundary layer that is capped by an inversion layer. The stirring mechanisms are the buoyancy flux due the heating of the ground by solar radiation and shear stresses due to horizontal winds. An inverse and somewhat more complicated situation occurs in the upper ocean layer. The buoyancy flux due to surface heat loss is also influenced by the salt content, the transfer of wind energy is effected by the excitation of waves. The situation is even more complex in lakes and reservoirs. Due to the limited size of a lake, recirculating flows and thermocline oscillations (seiches) may cause shear and hence produce turbulence at the side slopes of the bottom and along the interface. Absorption of radiation in the stratified layer, i.e. the hypolimnion, is no longer negligible and molecular diffusion may

play a role in the heat transport across the interface. These processes have been schematically depicted in Fig. 1-1.

Many researchers have attempted to derive quantitative relationships for the turbulent entrainment across an interface from theoretical considerations, from observations and from laboratory experiments. Their papers will be reviewed and evaluated in the following sections:

2.2 Basic Equations and Definitions

In order to interpret the research results on turbulent entrainment and to identify the different ways to produce, dissipate and transport TKE, it is useful to derive the balance equation of TKE for a horizontal layer first. (For more detailed derivations, see e.g. Turner (1973) or Phillips (1977)). It can easily be found by forming the scalar product of the momentum equation and the velocity vector $\vec{u}$. Applying the Boussinesq approximation and neglecting Coriolis terms, the momentum equation can be written as

$$\frac{d\vec{u}}{dt} = -\frac{1}{\rho_o}\nabla p + b\vec{m} + \nu\nabla^2\vec{u} \qquad (2\text{-}1)$$

(p = pressure deviation from the hydrostatic pressure, $b = -g\,\frac{\rho-\rho_o}{\rho_o}$ = buoyancy, where $\rho-\rho_o$ is the deviation from the reference density ρ_o, ν = kinematic viscosity, $\vec{m}$ = vertical unit vector).

All quantities that show turbulent fluctations, can be expressed in terms of a mean value and a fluctuating part: $\vec{u} = \vec{U} + \vec{u}'$, $p = P + p'$, $b = B + b'$. Forming the scalar product of equation (2-1) with the fluctuating velocity field $\vec{u}$, and then taking the probability average yields the equation of the TKE. In Cartesian tensor notation, it is

$$\left(\frac{\partial}{\partial t} + U_j\frac{\partial}{\partial x_j}\right)\frac{1}{2}\overline{u_i^2} + \frac{\partial}{\partial x_j}\overline{\left\{u_j\left(\frac{p}{\rho_o} + \frac{1}{2}u_i^2\right)\right\}} = -\overline{u_i u_j}\frac{\partial U_i}{\partial x_i} + \overline{bw} - \varepsilon \qquad (2\text{-}2)$$

with $i,j = 1,2,3$.

The bar denotes the average, the primes at the fluctuating parts have been dropped. Before explaining the single terms of eq. (2-2), several other simplifications will be applied. In situations under consideration, the mean flow is usually horizontal, and the turbulence can be taken as approximately homogeneous in horizontal planes. Assuming one coordinate in the direction of the main horizontal flow, eq. (2-2) reduces to

$$\frac{\partial}{\partial t}\overline{q^2} + \frac{\partial}{\partial z}\overline{\{w(\frac{p}{\rho_o} + q^2)\}} = -\overline{uw}\frac{\partial U}{\partial z} - \frac{g}{\rho_o}\overline{w\rho} - \varepsilon \qquad (2\text{-}3)$$

① ② ③ ④ ⑤

Here $\overline{q^2} = \frac{1}{2}\overline{(u^2 + v^2 + w^2)}$ is the TKE per unit mass.

Term 1 is the temporal change of TKE, while term 2, the divergence of the energy flux, specifies the redistribution of energy in the physical space by the turbulence itself. The terms on the right hand side represent the three ways in which TKE is either acquired or lost. Term 3 is the rate of transfer from the mean flow by the working of the Reynolds stress, $-\rho\overline{uw}$, against the mean velocity gradient. Term 4 stands for the gain or loss of TKE due to the release or increase of potential energy of the mean density field, depending on whether the stratification is unstable or stable. Since density fluctuations are small, a linear approximation for the equations of state between the density and the temperature can be assumed and the buoyancy flux term can also be written as $\frac{g}{\rho_o}\overline{w\rho} = -\alpha g\overline{w\theta}$, where θ is the temperature fluctuation and α is the thermal expansion coefficient. Term 5, ε, finally denotes the dissipation of TKE. While term 4 can have either sign, terms 3 and 5 are essentially positive.

For the evaluation of experiments or observations and for the theoretical treatment of turbulent entrainment, an idealized form for the turbulent mixed layer and the adjacent quiescent layer is usually assumed,

(Fig. 2-1). The mixed layer of a depth h is bounded by an interface of negligible thickness, represented by a density step $\Delta\rho$. The quiescent layer underneath (or above) has a linear density gradient Γ. (In some experiments, a homogeneous stagnant layer was used.) Due to the turbulence produced by the stirring mechanism (mechanical or buoyant), the mixed layer depth h increases by dh during a time interval dt. The quotient $u_e = \frac{dh}{dt}$ is called entrainment velocity.

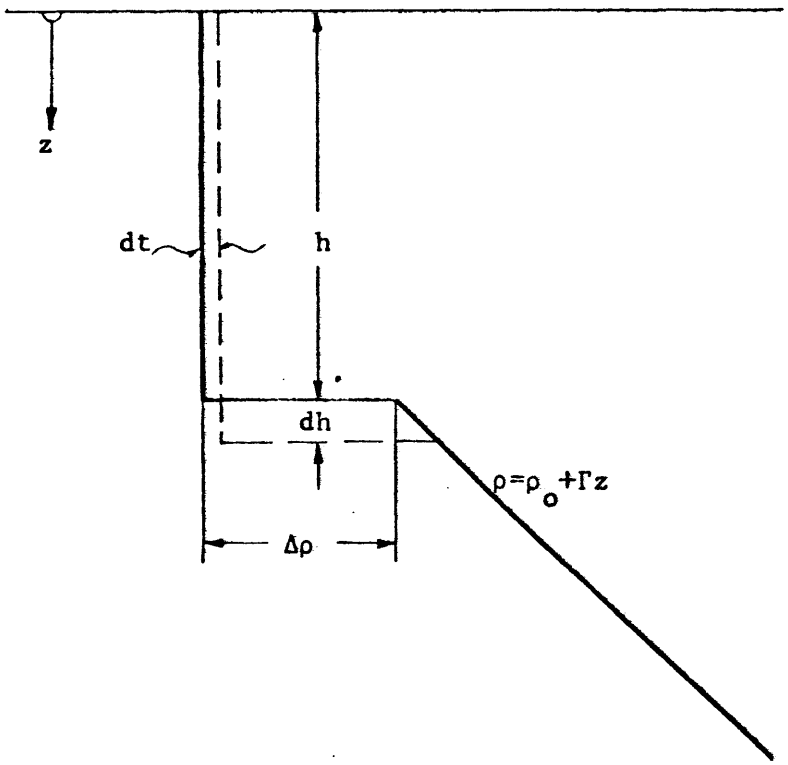

Fig. 2-1 Idealized Representation of Turbulent Entrainment at a Density Interface

2.3 Turbulent Entrainment Due to Mechanical Stirring

Most laboratory experiments that were carried out to study the turbulent entrainment process across a density interface used a mechanical stirring device to generate turbulence. The basic devices that were used in these experiments are shown in Fig. 2-2.

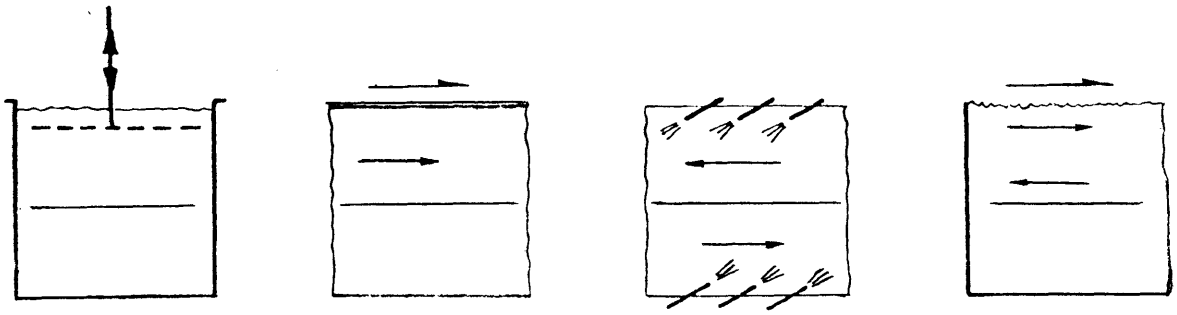

a) Turner (1968) b) Kato&Phillips (1969) c) Moore&Long (1971) d) Wu (1973)

Fig. 2-2 Turbulent Entrainment Experiments Using Mechanical TKE-Generation

Following the experiments of Rouse and Dodu (1955), Turner (1968) generated turbulence with an oscillating grid of solid bars, located at a fixed distance from an interface between two layers of water with different densities (Fig. 2-2a). The grid-interface distance was kept constant either by withdrawing fluid from one layer or stirring each layer with a grid, in which case the interface centered itself midway between the two grids. The density differences were created by different temperatures or by different salt contents in the two layers. Turner found that the entrainment velocity u_e, scaled with a turbulent velocity scale σ(the r.m.s. of the horizontal component of the turbulent velocity), is proportional to the inverse of a densimetric Richardson number Ri:

$$\frac{u_e}{\sigma} \propto Ri^{-1} \qquad (2\text{-}4)$$

The Richardson number was defined as $Ri = \frac{g \Delta\rho \ell}{\rho_0 \sigma^2}$, where $\Delta\rho$ is the density difference between the upper and lower layer and ℓ is a turbulent length scale. For higher Richardson numbers, however, the measurements from the salinity experiments were more closely related to $Ri^{-3/2}$:

$$\frac{u_e}{\sigma} \propto Ri^{-3/2} \tag{2-5}$$

Thompson and Turner (1975) measured the turbulent length and velocity scales using a hot-film technique. They found

$$\ell = 0.1z \tag{2-6}$$

$$\sigma = 1.4f \cdot z^{-3/2} \cdot s^{-5/2} \tag{2-7}$$

where z is the distance from the grid, f and s are the frequency and the stroke of the grid, respectively. Using these scales, Turners (1968) results are plotted in Fig. 2-3.

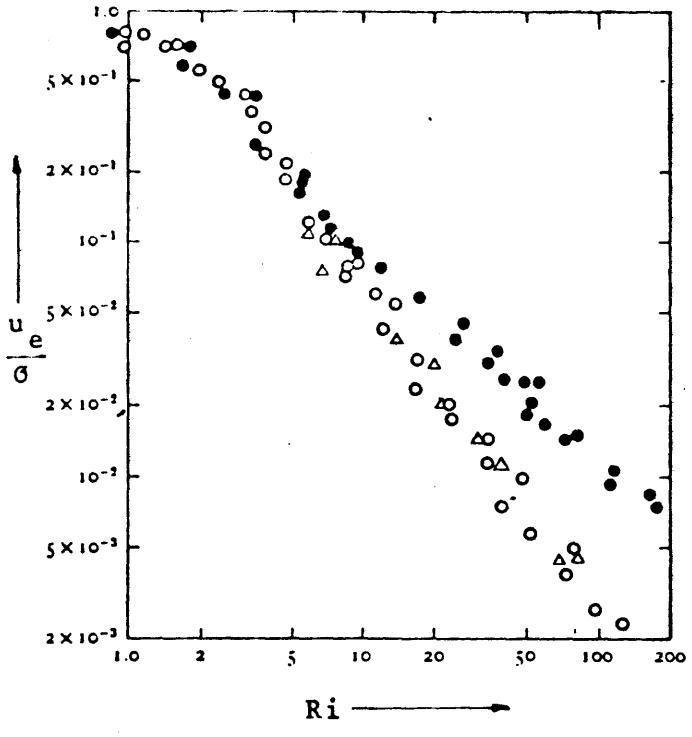

Fig. 2-3 Dependence of the Entrainment Velocity u_e on the Richardson Number Ri (•, ○ Turner (1973), Δ Hopfinger and Toly (1976))

Hopfinger and Toly (1976) found the same dependence of ℓ on the grid distance z and of σ on the stroke s in their experiments on grid-generated turbulent entrainment in a salinity stratified two-layered system, but variations in the mesh size, shape and stroke length of their grid yielded different relationships between σ and z. Their results are also plotted in Fig. 2-3, backing relationship (2-5).

Turner (1968) first tried to explain the different exponents in equations (2-4) and(2-5) in terms of the different molecular diffusivity of heat and salt. An energy argument (cf. chapter 2.5) led him to assume that the Ri^{-1} law is in some way fundamental, and that the salt flux is reduced because of a slower incorporation of an entrained element into its surroundings by diffusion. The experiments of Wolanski and Brush (1975) using different solutes with molecular diffusivities between 10^{-7} and 10^{-11} m^2/s and yielding Richardson number exponents up to -3, seemed to support this point of view. Because of different length and velocity scales, their results could not be included in Fig. 2-3. On the other hand, Linden(1973) concluded from observations of the entrainment process at the interface the $Ri^{-3/2}$ - relationship to be the universal law. He directed vortex rings towards a density interface. An energy balance describing the distortion and penetration of the vortex ring after the impact at the interface yielded the exponent -3/2. Turner (1973) later adopted this point of view. Linden (1975) also carried out experiments for a linearly stratified quiescent layer. In this case the exponent varied between -0.7 and -1.5.

Kato and Phillips (1969) have reported an entrainment experiment in an annular tank, where the turbulence was produced by a controlled constant shear stress τ applied to the surface of the upper turbulent layer

by a rotating screen. The lower layer was linearly stratified due to a salt gradient (cf. Fig. 2-2b). Their measurements suggest a relationship similar to eq. (2-4),

$$\frac{u_e}{u_*} = 2.5\ Ri_*^{-1} \tag{2-8}$$

The length and velocity scales are the mixed layer depth h (analogous to eq. (2-6)) and the friction velocity u_*, defined as $\tau = \rho_o u_*^2$. The constant of proportionality was found from a best fit of the experimental data (Fig. 2-4).

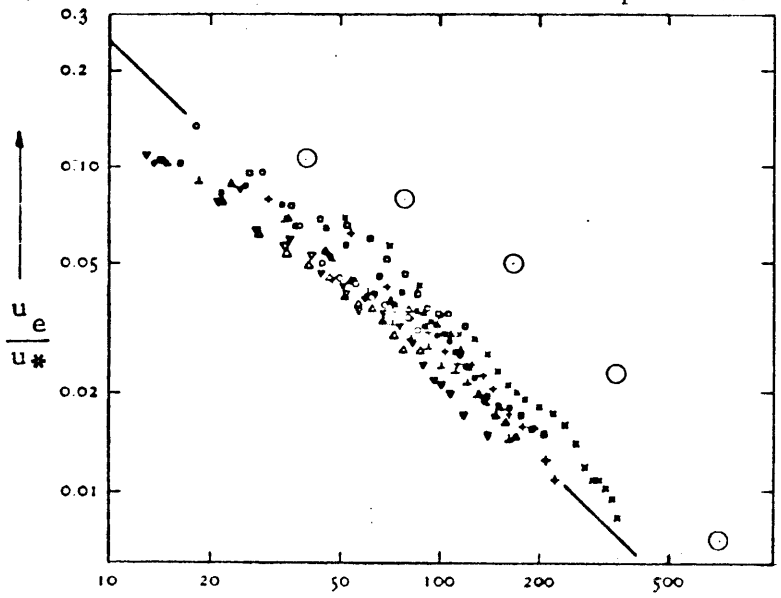

Fig. 2-4: Dependence of Entrainment Velocity u_e on the Richardson Number Ri_* (small symbols: Kato and Phillips (1969), large circles: Kantha, Phillips and Azad (1977)).

Kantha, Phillips and Azad (1977) used the same apparatus to carry out entrainment measurements in a two-layered fluid. They achieved higher entrainment rates than Kato and Phillips (1969). Their results (the size of the symbols in Fig. 2-4 correspond to the scatter of their measurements) suggest an exponent that is depending on the Richardson number. For low Richardson numbers (<100) the slope assumes values >-1 (suggesting a limiting value for u_e as Ri goes to zero), while for higher Richardson

numbers (>500), the entrainment velocity decreases quite rapidly (suggesting that for very strong stratification the interface acts like a rigid lid and entrainment ceases). Taking a closer look on the measurements by Kato and Phillips (1969) they seem to exhibit a similar tendency despite the scatter of the data. Some uncertainty exists about the absolute location of these relationships in the u_e - Ri - diagram, (i.e., the value of the constant in eq. (2-8)). Pederson (1977) and Wu (1978) claim that the shear stresses that were exerted by the side-walls on the rotating upper turbulent layer (and partially balance the surface shear stress applied by the screen) were not accounted for sufficiently by Kato and Phillips (1969) or Kantha et al. (1977), respectively.

Moore and Long (1971) investigated turbulent entrainment between two rotating layers in an oval tank (Fig. 2-2c) by ejecting jets into both layers in opposite directions. Their results support the Ri^{-1} dependence.

Wu (1973) simulated the wind-induced turbulent entrainment in a wind-wave tank (Fig. 2-2d). He also found that his entrainment velocities follow the Ri^{-1} - law, although his constant of proportionality is one order of magnitude smaller than the one given by Kato and Phillips (1969).

2.4 Turbulent Entrainment Due to Buoyancy Fluxes

In lakes and in the ocean, the mechanical stirring due to the wind stress acting on the surface is the main source for entrainment across the thermocline. However, buoyancy fluxes due to surface heat loss also can cause turbulent mixing, although their effect on entrainment is considered to be at least small (Turner (1973)). The growth of the atmospheric boundary layer into the capping inversion layer, on the other hand, is primarily caused by buoyancy fluxes resulting from absorption of radiation on the ground.

In this case no scaling velocity is given a priori. A different approach has, therefore, been taken to describe the turbulent entrainment on top of the turbulent layer. Betts (1973) model assumed that the buoyancy heat flux at the interface, ϕ_e (where ϕ is the actual heat flux Φ divided by the product of density and heat capacity ρc_p) is a constant fraction of the buoyancy heat flux at the ground, ϕ_o :

$$\frac{\phi_e}{\phi_o} = -k \qquad (2\text{-}9)$$

In the idealized case of negligible interface thickness, ϕ_e can be written as (Ball (1960))

$$\phi_e = -u_e \Delta T_i \qquad (2\text{-}10)$$

with ΔT_i denoting the temperature step across the interface[1].

In the early models two limiting cases were considered:

(a) The turbulence due to the buoyancy heat flux at the bottom is completely dissipated within the layer. No turbulent entrainment takes place and the temperature change in the mixed layer is only due to the heat input. In this case, $k = 0$, Lilly (1968).

(b) The buoyancy heat flux is mostly used for turbulent entrainment while the effect of heat input on the temperature change is almost negligible. This corresponds to high values of k, e.g. $k = 1$((Ball 1960), Lilly (1968)). Betts (1973) compared his analytical solution with experimental data and reported a value of $k = 0.25$.

Since then, many theoretical and experimental investigations and observations of the atmospheric boundary layer have been carried out to

---

(1) In atmospheric models, T stands not for the actual temperature, but the potential temperature referring to an adiabatic, that is, neutrally stratified environment.

determine the value of k. They were reviewed by Stull (1976) and, more recently by Denton (1978). Values for k, found by different researchers and by different methods (t = theoretical, e = experimental, o = observational) are listed in Table 2-1. The mean range of k appears to lie between 0.1 and 0.3.

Tennekes (1973) offered a simple physical interpretation for eq. (2-9). He evaluated the TKE balance equation (2-3) at the interface, assuming, that the transient term 1 and shear stress production (term 3) are negligible and that the dissipation term 5 is at least proportional to the divergence term 2 (or also negligible). The TKE balance then reduces to

$$\left(\frac{\partial}{\partial z}\ \overline{\left\{w\ (\frac{p}{\rho_o} + q^2)\right\}}\right)_i = -\left(\frac{g}{\rho_o}\ \overline{w\rho}\right)_i \quad = \quad (\alpha g\ \overline{w\theta})_i \tag{2-11}$$

where $-(\overline{w\theta})_i$ is equivalent to ϕ_e.

Tennekes (1973) argued that the large eddies which transport most of the kinetic energy scale on the r.m.s. vertical velocity fluctuation, σ, and on the mixed layer depth, h. Therefore, the divergence term can be estimated as

$$\left(\frac{\partial}{\partial z}\ \overline{\left\{w(\frac{p}{\rho_o} + q^2)\right\}}\right)_i \ \propto \frac{\sigma^3}{h} \tag{2-12}$$

The velocity scale was given by Deardorff (1970) as

$$\sigma^3 \propto \alpha g\ (\overline{w\theta})_o\ h \ = \ w_*^3 \tag{2-13}$$

where $(\overline{w\theta})_o$ is the buoyancy heat flux at the bottom, ϕ_o. Combining eqs. (2-11), (2-12) and 2-13) yields eq. (2-9):

$$-\ (\overline{w\theta})_i \propto (\overline{w\theta})_o$$

or

$$\frac{\phi_e}{\phi_o} \ = \ -k \tag{2-9}$$

TABLE 2-1. Published Values of the Heat Flux Ratio k

(t = theoretical, e = experimental (laboratory),
o = observational (atmospheric data))

Investigator	Year	Type	k	Comment
Ball	1960	t	1	Linear Stratification
Lilly	1968	t	0-1	"
Betts	1973	o.t	0.25	"
Carson	1973	o.t	0-0.5(0.25)	"
Tennekes	1973	t	0.2	"
Stull	1973	t	0.15	"
Readings	1973	o	0.2-0.3	"
Rayment & Readings	1974	o	(0.5)	"
Sacharik	1974	t	0.2	"
Deardorff	1974	t	0.14-0.21	"
Deardorff et al.	1974	e	0.23	"
Cattle & Weston	1975	t	0.29-0.32	"
Barnum & Rao	1975	t	0.35	"
Heidt	1975	e	0.18 ± 0.06	"
Jenkins	1974	e	0.35 ± 0.07	Two-layered
Denton & Wood	1974	e	0.2 - 0.5	"

The above parameterization can also be used to show that Eq. (2-9) is equivalent to the Ri^{-1} law found in several mechanical stirring experiments, e.g. the results of Kato and Phillips (1969). In that case, the velocity scale was the friction velocity u_*. Thus

$$(\overline{w\theta})_i \propto \frac{u_*^3}{\alpha g h}$$

Using eq. (2-10) for the buoyancy heat flux at the interface and setting $\alpha\Delta T_i = \Delta\rho/\rho_o$ yields eq. (2-4) or eq. (2-8).

$$\frac{u_e}{u_*} \propto \frac{\rho_o u_*^2}{g\Delta\rho h} = Ri^{-1} \qquad (2\text{-}14)$$

2.5 Summary of Turbulent Entrainment Models

The attractive physical interpretation of the Ri^{-1} law as an energy ratio, that was derived in the previous chapter, probably led many investigators to adopt it as the fundamental law. It can be restated as a balance between the kinetic energy input and the change of potential energy in the layer due to entrainment. Using the notation defined in Fig. 2-1, the change of potential energy due to the entrainment of a fluid element of the thickness dh is

$$dE_{pot} = Adh\Delta\rho g\frac{h}{2} \qquad (2\text{-}15)$$

(A = surface area)

The input of (turbulent) kinetic energy during that time for the case that shear stress is applied to the surface, is

$$dE_{kin} = \tau u_s \, dt \, A \qquad (2\text{-}16)$$

where u_s is the drift velocity of the surface. As shown in section 3.3, the drift velocity u_s is usually very close to the friction velocity u_*. Eq. (2-16)

can be reformulated as

$$dE_{kin} = \rho_o u_*^3 dt\, A \qquad (2\text{-}17)$$

where $u_s = u_*$. Combining eqs. (2-15) and (2-17), i.e., assuming that the kinetic energy is completely transferred into potential energy, yields

$$\frac{dh/dt}{u_*} = 2\,\frac{\rho_o u_*^2}{g\Delta\rho h} \qquad (2\text{-}18a)$$

or

$$\frac{u_e}{u_*} = 2\ Ri^{-1} \qquad (2\text{-}18b)$$

Relationship (2-18a) was used in the original version of the wind-mixing subroutine of the MIT-model to account for wind-induced entrainment across the thermocline.

Although many experiments and observations seem to support the Ri^{-1} law, the scattering of data in experiments, the uncertainty about the constant of proportionality in eq. (2-4) or about the value of k in atmospheric models, and the limited range of Richardson numbers (usually less than one decade), over which the different experiments were carried out, cast some doubt on the general validity of this simple law. In fact, the experiments by Kantha et al. (1977) covering a Richardson number range of two decades indicate that an exponent of -1 is only appropriate for Richardson numbers of about 200. Turner (1968) already pointed out that for low Richardson numbers, the entrainment velocity approaches a constant value (instead of infinity as predicted by the Ri^{-1} law), that is related to the finite propagation velocity of a turbulent front in a homogeneous layer. On the other side, the rapid decrease of the entrainment velocity for high Richardson numbers may be explained by the fact that the interface acts as a rigid lid, if the adjacent layer is very strongly stratified.

In general, two explanations can be given for the apparent lack of agreement between the various models. One reason is the insufficient verification of the idealized model (Fig. 2-1) in experiments and in nature.

The density step of negligible thickness is partially eroded by molecular diffusion. This led Turner (1968) to suggest a more general relationship for the entrainment velocity, including a Péclet number $Pe = \frac{\sigma \ell}{\kappa}$, where κ is the molecular diffusivity: $u_e/\sigma = f\ (Ri,Pe)$. In addition, under natural conditions, the initial condition inherent in the models, i.e., a linearly stratified layer, is often not verified.

The second reason is that the simple balance between TKE input and change in potential energy as given in eq. (2-18) is representative only for situations with intermediate stratification. For very weak or very strong stratification other mechanisms of TKE-transfer or conversion seem to be no longer negligible in the TKE - balance. This will be discussed in detail in the next chapter.

III. Formulation of a Wind-Mixing Algorithm

3.1 Parameterization of the TKE-Balance

The literature review in the previous chapter has shown that the formulation of an entrainment law as a balance between the divergence term and the buoyancy term in eq. (2-3) is insufficient, at least for certain situations. Transient and dissipation effects may play a role in some parts of the Richardson number domain. Zeman and Tennekes (1977) were among the first to parameterize all terms of the TKE-equation (2-3) expanding an earlier paper of Tennekes (1973) and comment to that paper by Zilitinkevich (1975). They evaluated this equation at the density interface:

$$\left(\frac{\partial \overline{q^2}}{\partial t}\right)_i + \left(\frac{\partial}{\partial z}\left\{w\left(\frac{\overline{p}}{\rho_o} + \overline{q^2}\right)\right\}\right)_i = \left(-\overline{uw}\,\frac{\partial u}{\partial z}\right)_i - \left(\frac{g}{\rho_o}\,\overline{w\rho}\right)_i - \varepsilon_i \qquad (3\text{-}1)$$

The parameterization of the divergence term has already been described in Chapter 2.4 (Tennekes (1973)):

$$-\left(\frac{\partial}{\partial z}\left\{w\left(\frac{\overline{p}}{\rho_o} + \overline{q^2}\right)\right\}\right)_i = C_F\,\frac{\sigma^3}{h} \qquad (3\text{-}2)$$

Zilitinkevich (1975) pointed out that, for weak stratification and as a result, rapid propagation of the turbulent front, the transient term is no longer negligible. In this case, the input of turbulent kinetic energy is mainly used to increase the TKE content of the growing mixed layer, while the buoyancy flux across the interface is very small. He proposed

$$\frac{\partial \overline{q^2}}{\partial t} = -\frac{\partial \overline{q^2}}{\partial z}\cdot\frac{dh}{dt} = C_T\,\frac{\sigma^2}{h}\,\frac{dh}{dt} \qquad (3\text{-}3)$$

using the same length and velocity scales as Tennekes (1973). For a neutrally stratified environment ($\Gamma = 0$), the righthand side of eq. (3-1) becomes zero (if no mean shear is present) and the left-hand side can be

rewritten as

$$\frac{dh}{dt} = \frac{C_F}{C_T} \sigma \qquad (3\text{-}4)$$

This corresponds to the expected finite "entrainment" velocity in an unstratified environment that is proportional to the turbulent intensity σ in the turbulent layer.

For the dissipation of TKE two possible mechanisms are considered. If the kinetic energy loss is caused by a turbulent energy cascade process, it can be parameterized as

$$\varepsilon_i = C_D \frac{\sigma^3}{\ell} \qquad (3\text{-}5)$$

where ℓ is a length scale for the turbulence near the interface (Batchelor 1953)). An obvious choice would be to take ℓ proportional to the mixed layer depth h; however, this would make the dissipation rate proportional to the divergence term (eq. 3-2) and only result in a reduction of the coefficient C_F, that is determined from experimental data. In this way dissipation was accounted for in Denman's (1973) model of the upper ocean.

A second possible dissipation mechanism is the loss of TKE associated with the radiation of internal wave energy into the adjacent stably stratified layer. According to Linden (1975) this mechanism can also be parameterized by eq. (3-5), if a suitable choice is made for the length scale ℓ. Zeman and Tennekes (1977) suggested the height to which eddies with a velocity proportional to σ can penetrate into the stably stratified environment, as an appropriate length scale. If the density jump at the interface is small, this height can be calculated from a simple energy balance:

$$g \Gamma \ell^2 \propto \rho_o \sigma^2 \qquad (3\text{-}6)$$

Hence, the parameterization of the dissipation term is

$$\varepsilon_i = C_D \sigma^2 N \qquad (3\text{-}7)$$

where $N = (g\Gamma/\rho_o)^{1/2}$ is the Brunt-Väisälä frequency of the environment with a density gradient Γ.

The remaining term, the mechanical TKE production due to shear stress, contributes to the TKE balance evaluated at the interface only if the mean velocity gradients are large near the thermocline. This is usually not the case in lakes and reservoirs. Only during strong seiching motions, the shear stress across the thermocline could be appreciable. For this case, Zeman and Tennekes (1977) assume that the TKE produced by shear stress at the interface is used primarily to feed the local dissipation cascade, i.e. that the mechanical production term 3 and the dissipation term 5 are cancelling each other. This relation as well as the parameterization of dissipation in eq. (3-7) will be used for the formulation of the wind-mixing algorithm, but the emphasis will be on situations when shear stress at the thermocline is negligible.

During the previous derivations the length and velocity scales ℓ and σ have been specified in terms of measurable bulk quantities. The length scale was either set equal to the mixed layer thickness h (eq. (3-2), (3-3)) or was expressed in terms of the stratification of the quiescent layer (eq. (3-6)). The velocity scale σ was related to the boundary heat flux (and denoted as w_*) if the TKE input was due to buoyancy (eq. (2-13)), or to the friction velocity u_*, if it was caused by shear stress at the surface (eq. (2-14)). In general, both kinds of TKE production are present in lakes, the ocean or the atmosphere, so that σ has to be expressed as a function of both, w_* and u_*. Zeman and Tennekes (1977) assumed that

the total kinetic energy is a linear combination of the convective and mechanical contributions

$$\sigma^2 = w_*^2 + c^2 u_*^2 \qquad (3\text{-}8)$$

(Sherman et al. (1978) added the cubes, which is equivalent to adding transfer rates of TKE, following Kraus and Turner (1967)). However, the MIT-Lake and Reservoir model considers convective and shear-induced mixing in two separate subroutines. The wind-mixing algorithm only accounts for wind-driven mixing. The appropriate velocity scale is, therefore,

$$\sigma = c u_* \qquad (3\text{-}9)$$

The TKE-balance can now be expressed in a parameterized form (combining eq. (3-1), (3-2), (3-3), (3-7) and (3-9) and neglecting the shear stress term)

$$C_T \frac{c^2 u_*^2}{h} \frac{dh}{dt} = C_F \frac{c^3 u_*^3}{h} - \frac{g}{\rho_o} (\overline{w\rho})_i - C_D c^2 u_*^2 N \qquad (3\text{-}10)$$

$(\overline{w\rho})_i$ can be expressed as $\Delta\rho \frac{dh}{dt}$ (using eqs. (2-10) and (2-11)), and the Brunt-Väisälä frequency is given by $N^2 = g\Gamma/\rho_o = 2\frac{g}{h}\frac{\Delta\rho}{\rho_o}$, if the whole environment was initially linearly stratified. Then, eq. (3-10) can be reformulated into a u_e - Ri relationship:

$$\frac{u_e}{u_*} = \frac{cC_F - C_D\sqrt{2Ri}}{C_T + Ri/c^2} \qquad (3\text{-}11a)$$

where $u_e = \frac{dh}{dt}$ is the entrainment velocity and $Ri = \frac{g\Delta\rho h}{\rho_o u_*^2}$ is the Richardson number. For low Richardson numbers, i.e. weak stratification, the entrainment velocity approaches a constant value as predicted by Zilitinkevich (1975) (eq. (3-4)). As the stratification and hence the Richardson number increases, dissipation becomes more and more important. The entrainment decreases faster than predicted by the Ri^{-1} law. As the numerator becomes zero for a certain Richardson number, entrainment ceases completely.

If shear stress at the interface becomes appreciable and balances the local dissipation, the u_e-Ri relationship becomes

$$\frac{u_e}{u_*} = \frac{cC_F}{C_T + R_i/c^2} \tag{3-11b}$$

The relation yields the same limiting entrainment velocity for low Richardson numbers as eq. (3-11a), but approaches the Ri^{-1} law for higher values.

Zeman and Tennekes (1977) used the results of the convection experiments by Willis and Deardorff (1974) to determine the flux, dissipation and transient term constants C_F, C_D and C_T. The velocity scale w_* was calculated from the bottom heat flux, that caused the turbulent entrainment. They then fitted eqs. (3-11a and b) to Kato and Phillips' (1969) shear stress data to evaluate the constant c. Their best fits correspond to the following values: $C_F = 0.5$; $C_D = 0.024$; $C_T = 3.55$; $c = 2$. These values will be used for the formulation of the wind-mixing algorithm.

3.2 Wind-Mixing Algorithm

In Chapter 2.5 it has been shown that the Ri^{-1} law is equivalent to the rule that the increase of potential energy of the system due to entrainment is a constant fraction of the input of turbulent kinetic energy at the boundary

$$\frac{\Delta E_{pot}}{\Delta E_{kin}} = C \tag{3-12}$$

The previous wind-mixing algorithm (Hurley Octavio et al., 1977) was based on this relation with a value of C = 1, i.e., the total kinetic energy input was used for entrainment. For use in a finite difference scheme eqs. (2-15) and (2-17) can be written as

$$\Delta E_{pot} = A \, \Delta \, z \Delta\rho \, g \cdot \frac{m}{2} \Delta Z \tag{3-13}$$

where Δz is the element thickness, $h = m\Delta z$ the mixed layer thickness (consisting of m elements) and $\Delta\rho$ is the density difference between the mixed

layer and the adjacent layer below and

$$\Delta E_{kin} = \rho_o u_*^3 A \Delta t \qquad (3\text{-}14)$$

The applied procedure was to calculate the increase of potential energy by mixing the two top layers and to compare this amount to the input of kinetic energy during the time step Δt. If there was a surplus of kinetic energy, the two layers were mixed and the procedure was repeated for the next lower layer with the kinetic energy left. Once this remainder is too small to entrain the whole next layer, only part of this layer is mixed into the homogeneous layer. This part, with the new temperature of the homogeneous layer, is then mixed with the rest of the layer at its original temperature to fit into the numerical scheme again. Eqs. (3-13) and (3-14) imply that only TKE available at the cross-sectional area of the interface is used for entrainment, while the rest in the mixed layer above is used for redistribution and otherwise dissipated at the bottom (Hurley Octavio et al. (1977)).

If Eqs. (3-11a) or (3-11b) are multiplied by a Richardson number as defined in eq. (2-14), these equations can be written in a similar form as eq. (3-12)

$$\frac{\Delta E_{pot}}{\Delta E_{kin}} = f\,(Ri) \qquad (3\text{-}15)$$

(u_e is expressed as $\Delta h/\Delta t$)

Using the values for C_F, C_D, C_T and c found by Zeman and Tennekes (1977), the function f(Ri) can be evaluated quantitatively:

$$f(Ri) = 0.057\ Ri\ \{\frac{29.5\ -\ \sqrt{Ri}}{14.2\ +\ Ri}\} \qquad (3\text{-}16a)$$

if dissipation is considered (eq. (3-11a)), and

$$f(Ri) = \frac{Ri}{14.2\ +\ Ri} \qquad (3\text{-}16b)$$

if dissipation is balanced by mechanical production of TKE.

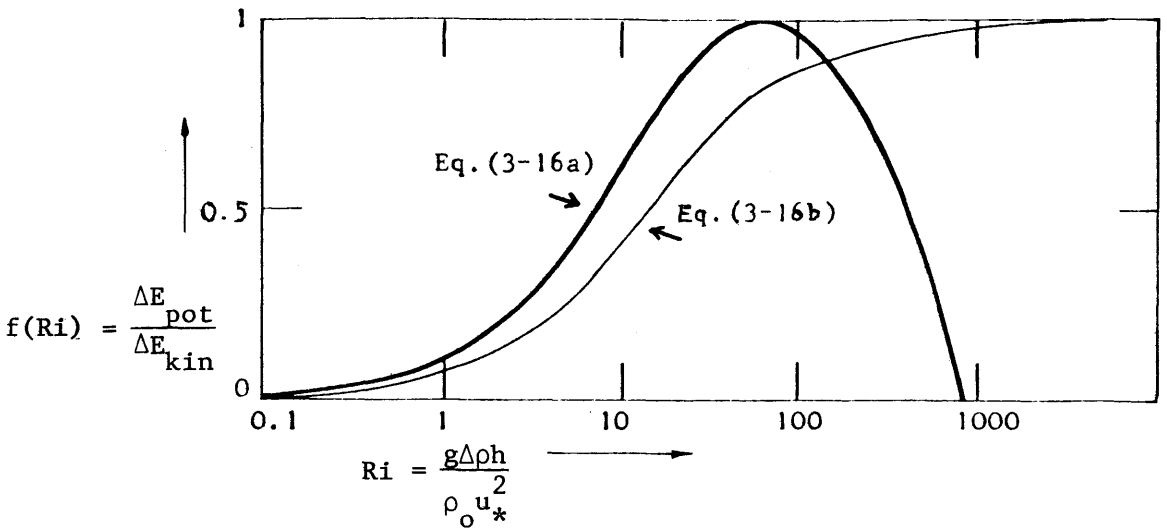

Fig. 3-1 Dependence of the Conversion of TKE into Potential Energy on the Richardson Number

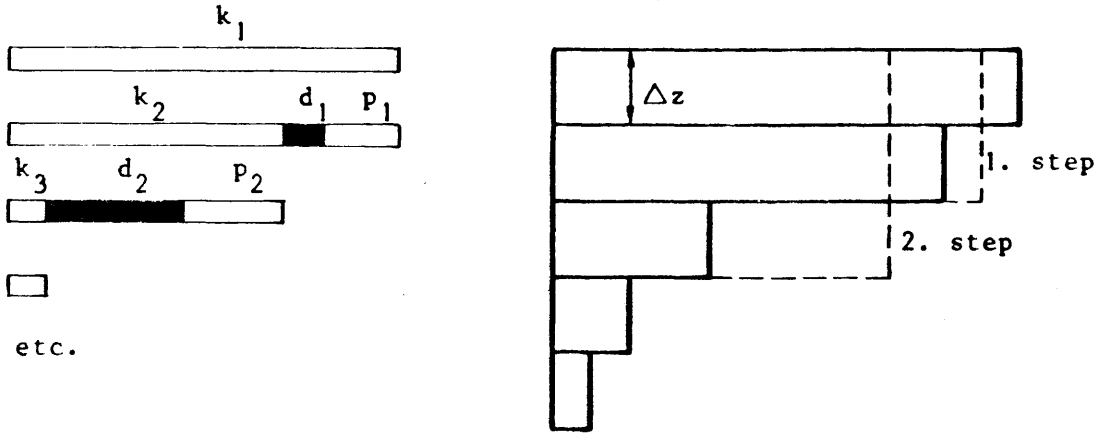

Fig. 3-2 Scheme of the Wind-Mixing Algorithm

The equations have been adjusted so that f(Ri) does not exceed unity. Both equations are shown in Figure 3-1. For low Richardson numbers, most of the kinetic energy input is used to increase the content of TKE of the mixed layer, while for higher Richardson numbers most of it is dissipated (eq. (3-16a)). Only for intermediate values of the Richardson number is the entrainment process efficient.

Equations (3-16 a and b) have been incorporated into the wind-mixing algorithm. The resulting procedure for eq. (3-16a) is schematically shown in Figure 3-2. In the first step, a part p_1 of the kinetic energy input k_1 is used to mix the first two layers. But in addition, the amount d_1 of the kinetic energy input k_1 is lost due to dissipation or increase of kinetic energy content of the mixed layer. Its magnitude is calculated from eq. (3-16a). In the second step, the same procedure is repeated for the amount of energy k_2 that is left. Evenutally the remainder becomes too small to entrain the whole next layer. Then, the partial mixing rule as described above is applied. The functional form given by eq. (3-16a) has been used for the case studies in Chapter 4. Equation (3-16b) has been applied for sensitivity studies in Section 5.4.

Some simplifications and inaccuracies that are inherent in the algorithm should be kept in mind when the algorithm is to be applied. First, the accuracy of the constants C_F, C_T, C_D and λ is probably less than $\pm 10\%$ due to scattering of the experimental data used for their determination. Second, the idealized form of the interface and the initial condition of a stratified layer, on which the entrainment model is based are usually not given in a lake or reservoir under natural conditions. Stable stratification up to the surface (although not linear) may develop on some days during early

summer, but mostly the upper layer is already mixed due to surface heat loss when wind-mixing is applied. The shape of the density profile at the thermocline is rather smooth than stepwise. Third, due to the discretization in the numerical scheme, the density step $\Delta\rho$ at the interface, that determines the Richardson number, and hence the dissipation rate, becomes dependent on the grid spacing Δz and, possibly, on the time step Δt. It will be examined during the application of the algorithm in Chapter V, whether or not these shortcomings affect the prediction capability of the algorithm.

3.3 Transfer of Kinetic Energy Across the Water Surface

The flux of kinetic energy across the lake-atmosphere interface can be described as the product of the shear stress τ exerted on the water surface by the wind and the drift velocity u_s of the surface water, as given in Chapter 2.5

$$\frac{1}{A}\,\frac{dE_{kin}}{dt} = \tau u_s = \rho_o u_*^2 u_s \qquad (3\text{-}17)$$

where u_* is the friction velocity of the water.

Unfortunately, eq. (3-17) cannot be used directly to calculate the energy input for the wind-mixing algorithm, because τ and u_s are difficult to measure and not available on a daily basis. It has therefore been attempted to relate these quantities to the wind field above the lake, e.g. to the wind speed at a given height. Despite the extensive research on this field, there still exists considerable uncertainty about the appropriate form of these relationships.

In general, the water surface is not rigid, but undulated due to the applied shear stress. Part of this wind stress is therefore used for the drag of longer waves. Estimates of this part, τ_w, differ considerably,

but Hasselmann et al. (1973) have evaluated oceanographic data and found a value of $\tau_w / \tau = 0.2$. In a lake, long wave trains are less likely to occur and the above ratio will be even smaller. It is assumed that the total momentum flux across the surface is used for TKE production via breaking of small waves or direct viscous shear, i.e. that the shear stress across the water surface is continuous: $\tau = \rho_o u_*^2 = \rho_a u_{a*}^2$ where the subscript a refers to the ambient air.

The total wind shear can now be related to the wind velocity W_Z at a given height Z by means of a momentum transfer coefficient C_Z (drag coefficient, friction coefficient)

$$\tau = \rho_o u_*^2 = C_Z \rho_a W_Z^2 \qquad (3\text{-}18)$$

Various measurements of C_{10} (where 10m has been adopted as standard reference height) have been reviewed recently by Busch (1977), Svensson (1978) and Coantic (1978). The measurements show some dependance of C_{10} on the wind speed W_{10}, but due to the wide scattering of data, Svensson (1978) suggested a value $C_{10} = 1.3 \cdot 10^{-3}$ as a good average. Coantic (1978) summarized his review with a linear relationship: $C_{10} = (1+0.05W_{10}) \cdot 10^{-3}$. Careful examination by recent investigators of the effect of (stable, neutral or unstable) stratification of the ambient air has made it possible to bring down the scattering.

The relationship between the friction coefficient C_Z and the wind spread W_Z that is used in the MIT model is based on the assumption of a continuous and constant shear stress at the water surface. Following Turner (1977), the wind speed distribution above the water surface can then be described by the well-known logarithmic profile:

$$W_Z = \frac{u_{a*}}{k} \ln \left(\frac{Z}{Z_0}\right) \qquad (3\text{-}19)$$

where k = 0.42 is v. Kármán's constant and Z_o is the roughness length (giving the virtual origin of the profile). On dimensional grounds, Charnock (1955) suggested

$$Z_o = 1.1 \cdot 10^{-2} \, u_{a*}^2/g \tag{3-20}$$

The combination of eqs. (3-18), (3-19) and (3-20) yields

$$\frac{1}{\sqrt{C_Z}} = \frac{1}{K} \ln \frac{gZ}{0.011 C_Z W_Z^2} \tag{3-21}$$

(This equation has also been suggested by Wu (1971))

From eq. (3-18) and (3-21) the shear stress τ can then be calculated.

Madsen (1977) and Kondo et al. (1979) have calculated the drift velocity u_s at the ocean surface and found it to be one order of magnitude larger than the water friction velocity. Wu (1973) got similar results in his wind-wave tank experiments. In both cases, a steady wind over a long period was assumed or applied. In a lake, winds change magnitude and direction more frequently. In addition, the fetch is limited, and a much smaller surface drift of the same order as u_* can be expected. For the calculation of the kinetic energy input in the MIT model, $u_s = u_*$ was used.

IV Application of the MIT-Lake and Reservoir Model

4.1 Lake 226NE, 1975

Lake 226 NE is the north-eastern basin of a two-lake system that is located in the Experimental Lakes Area in south-western Ontario near the town of Kenora. The two lakes are connected by a shallow channel, about 50m wide and less than 3m deep; however, interaction between the two lakes is prevented by curtains stretched across the channel. (Fig. 4-1) Lake 226NE can therefore be treated as a separate lake. It has approximately rectangular shape of about 400m by 200m (surface area: $8.3 \times 10^4 m^2$), the maximum depth is 14.7m (volume: $4.7 \times 10^5 m^3$).

Temperature profiles have been measured at the location of maximum depth in two-week intervals. Meteorological data, air temperature, relative humidity, wind speed (measurement height 13.2m), cloud cover and global radiation, were provided by a nearby meteorological station on a daily basis. In addition, daily measurements of the extinction coefficient were taken. In- and outflows were very small and were neglected in the calculations. Due to the lack of radiation measurements during May 1975, simulations could not be started before June 9, 1975. The measured temperature profile of this day was taken as initial condition. The time step was $\Delta t = 1$ day, the grid points were $\Delta z = 0.5$m apart. In eq. (1-3a), $\beta = 0.5$.

The results are shown in Fig. 4-2. Three different versions of the MIT model were used to calculate temperature profiles. For the dashed lines, no wind mixing was considered, i.e. molecular diffusion was the only vertical transport mechanism. The thin line corresponds to the previous wind-mixing algorithm, where the input of kinetic energy was completely transferred into potential energy, while the bold line shows the results of the new algorithm accounting for dissipation and transient effects.

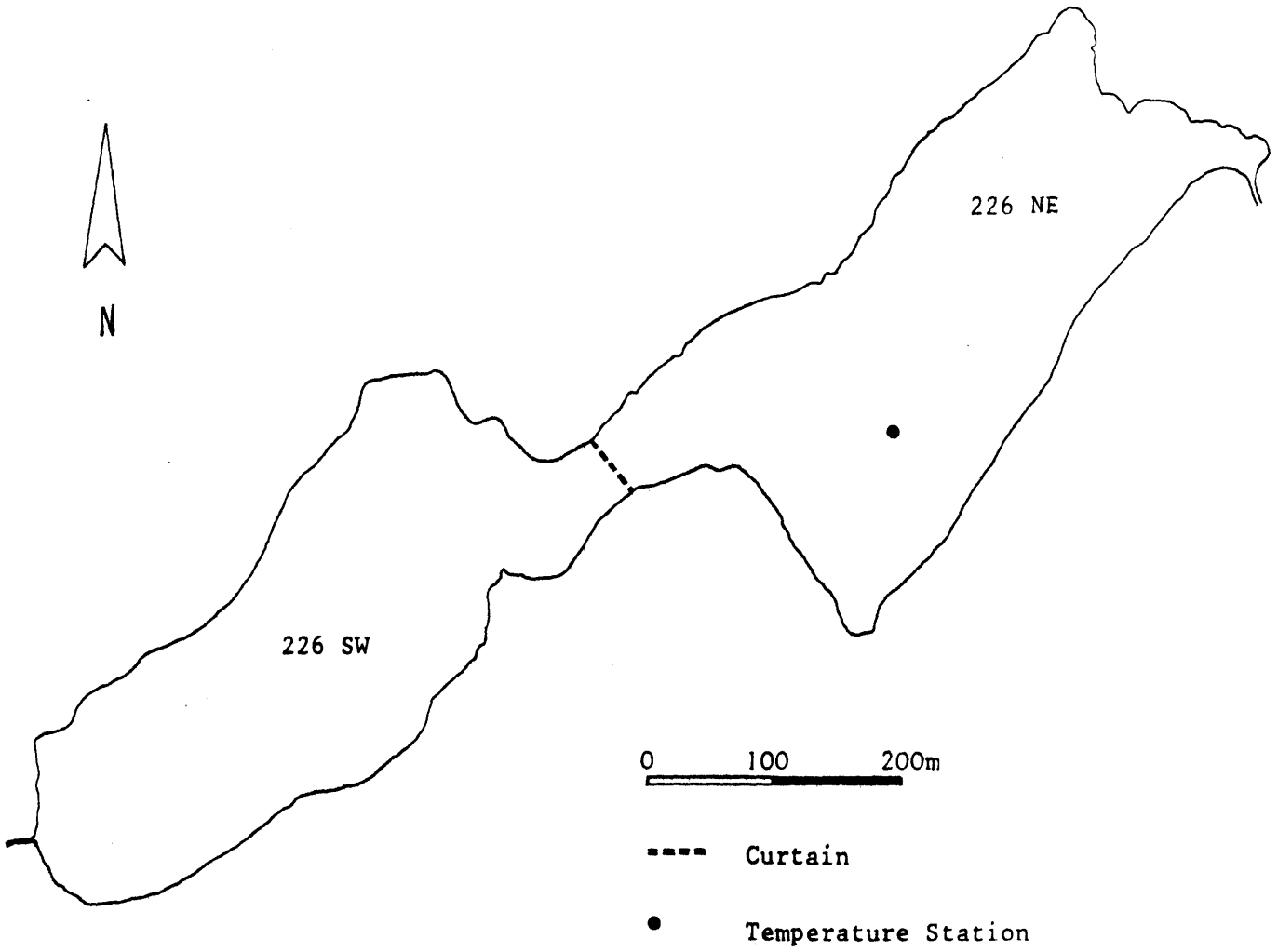

Fig. 4-1 Map of Lake 226, Ontario

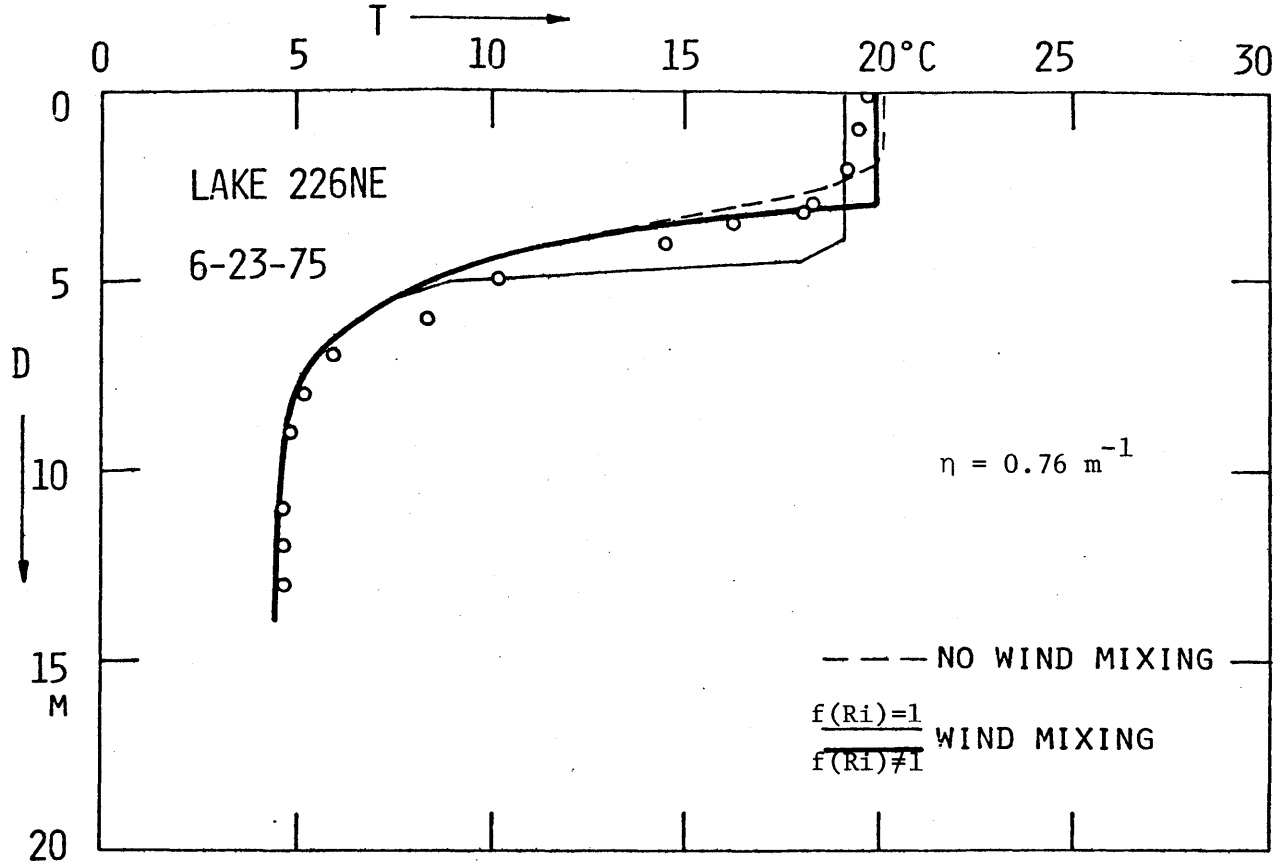

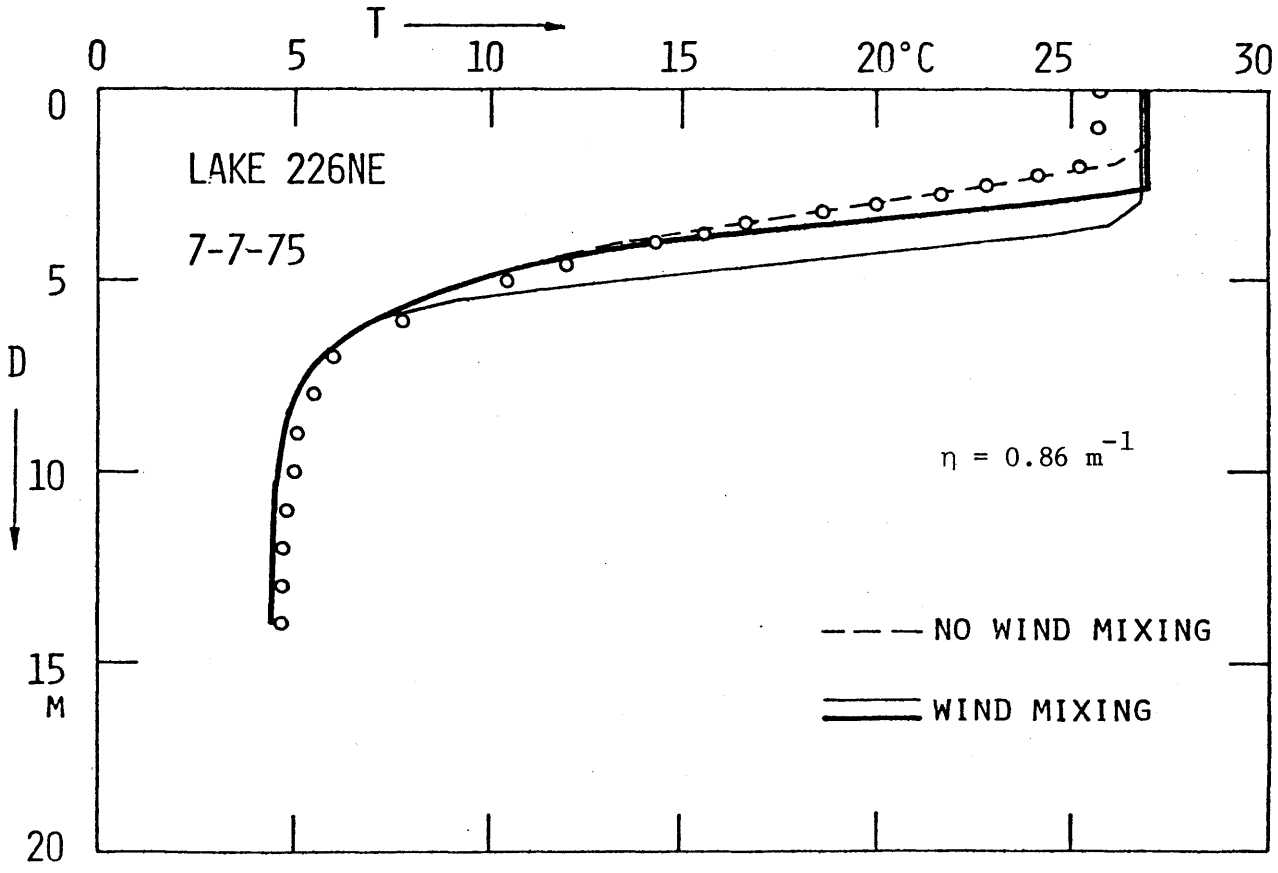

Fig. 4-2 Temperature Predictions for Lake 226NE, Ontario

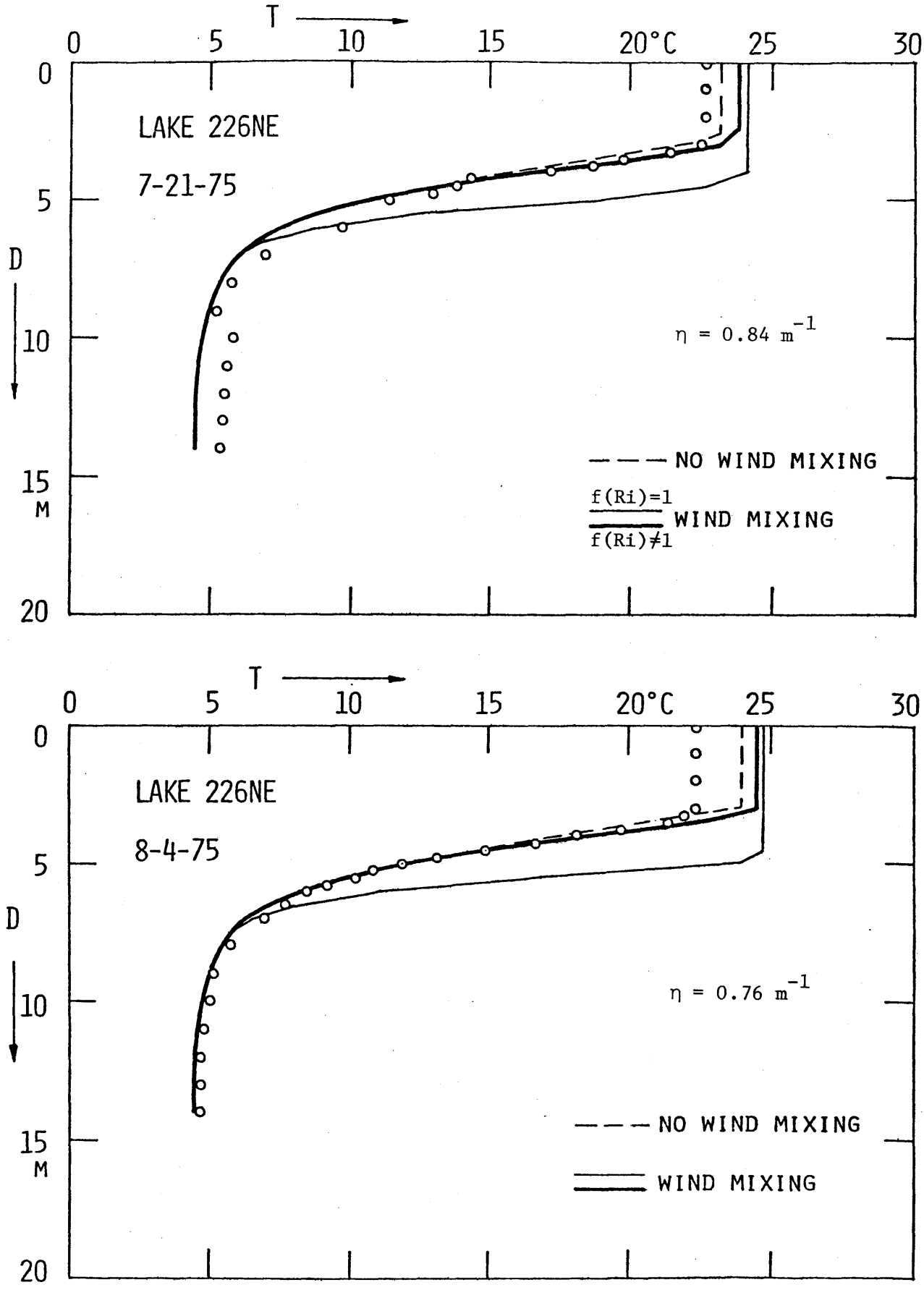

Fig. 4-2 (Continued)

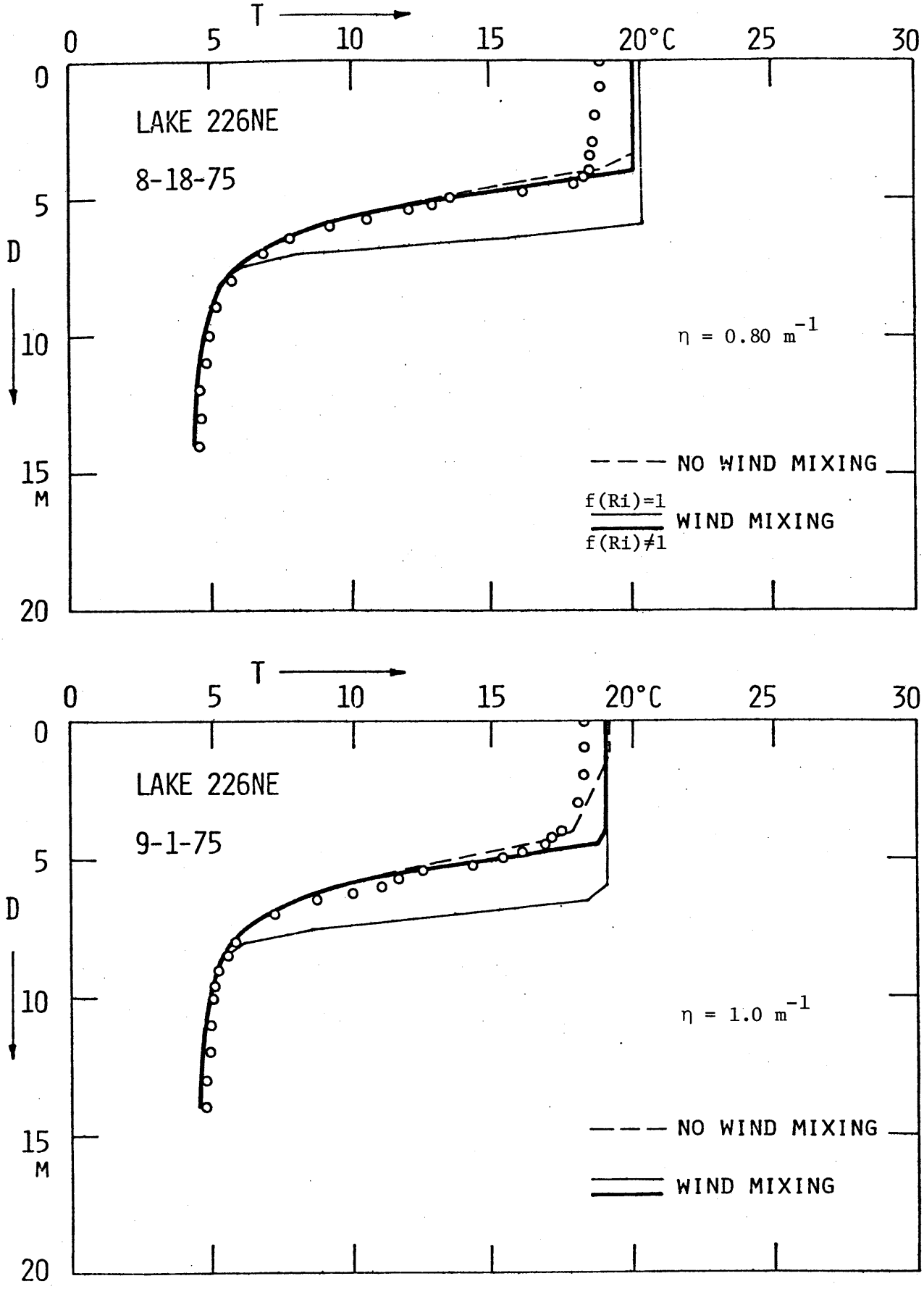

Fig. 4-2 (Continued)

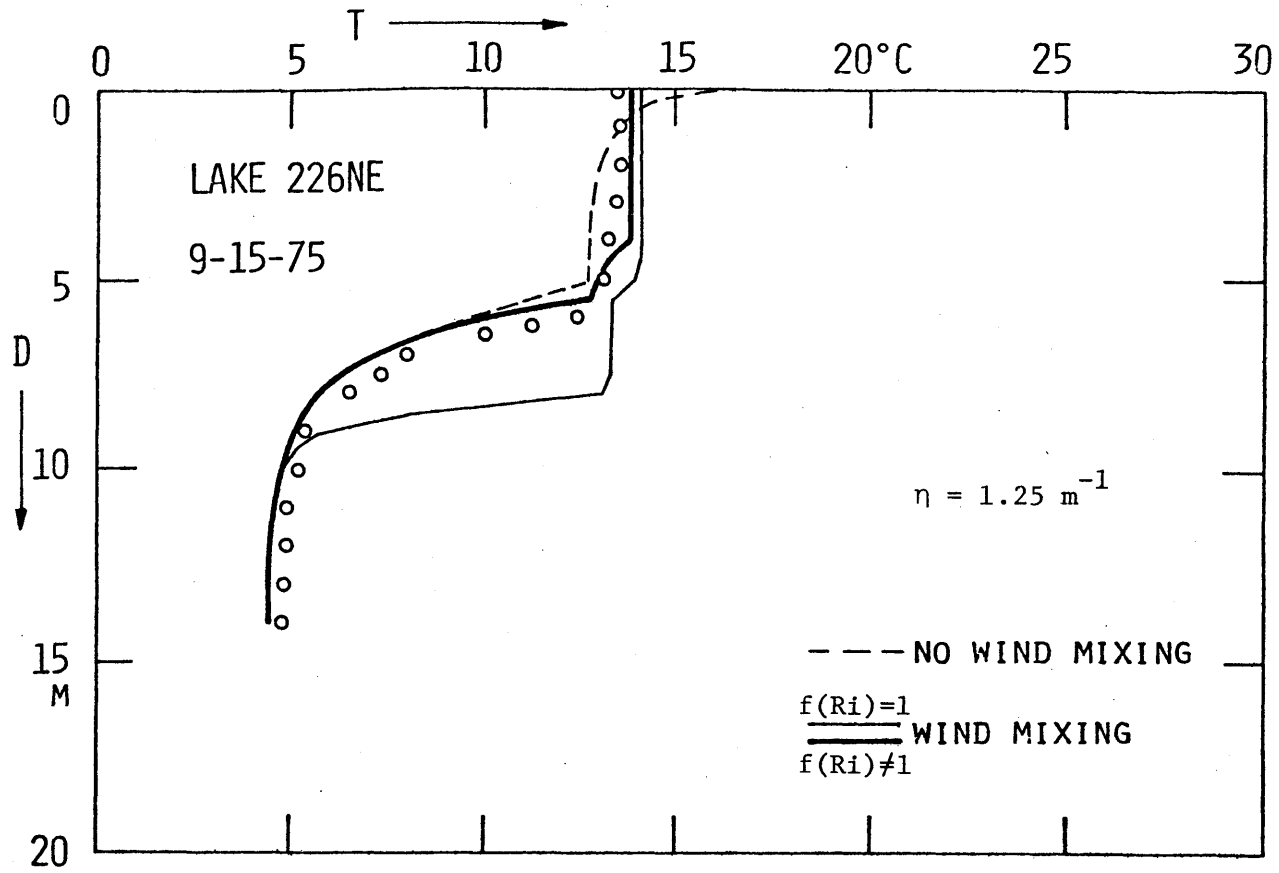

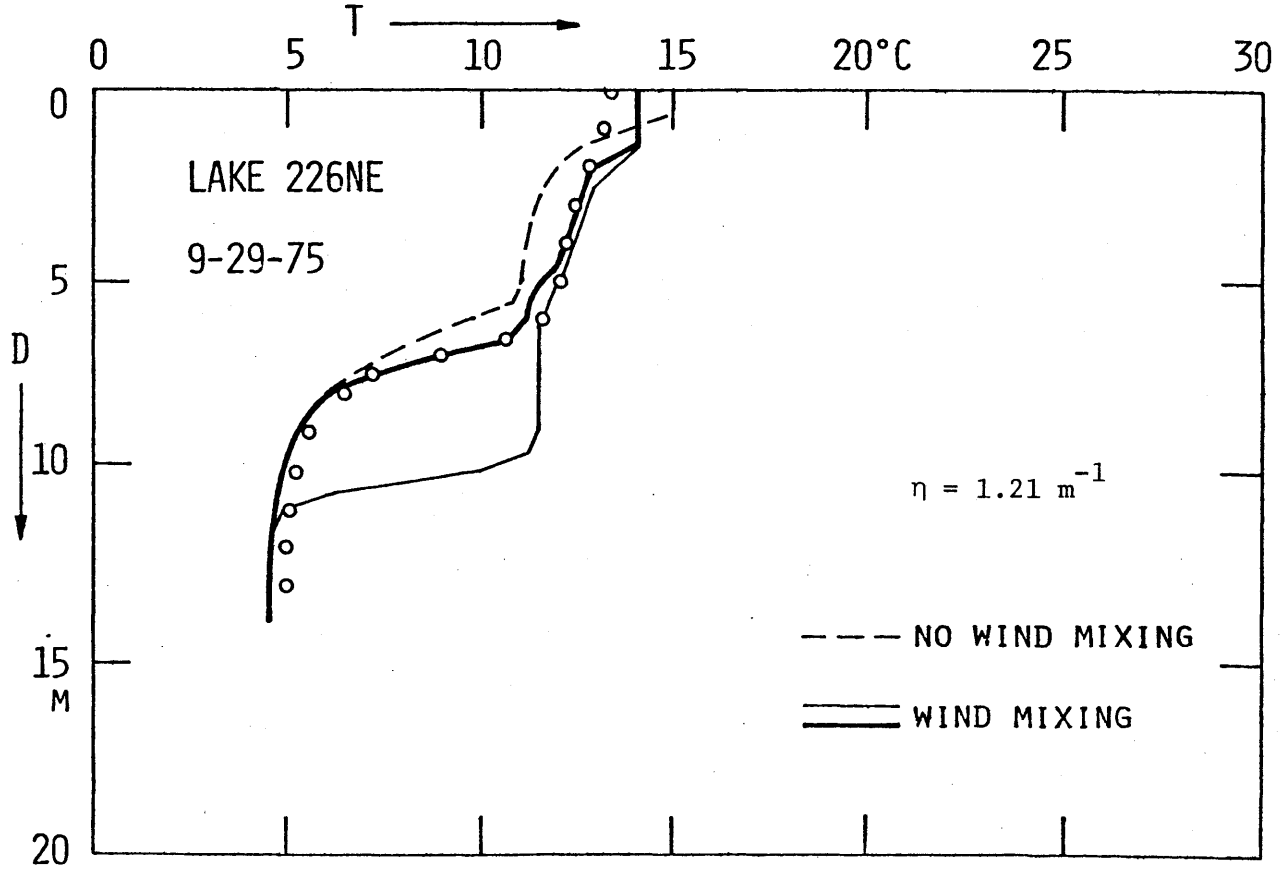

Fig. 4-2 (Continued)

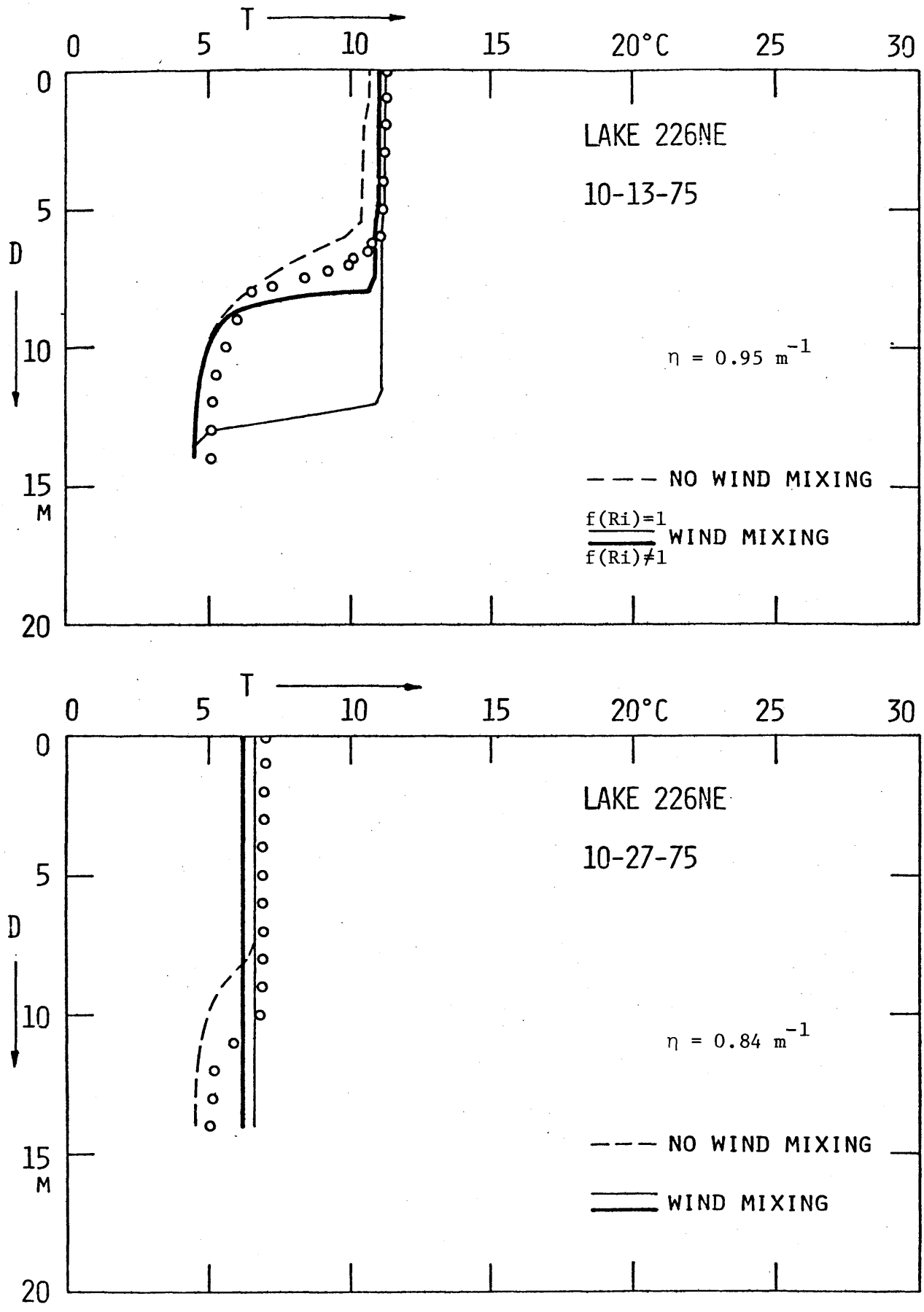

Fig. 4-2 (Continued)

In general, the agreement between measurements and predictions of the new algorithm is very good. During the summer, until the end of August, the prediction quality of the no-wind-mixing version is as good as the new algorithm. The reason is that the starting profile on June 9, 1975 was already strongly stratified, including possible mixing events during spring that would not be predicted without wind-mixing. Once, however, a strong gradient has developed, the only vertical transport mechanism seems to be molecular diffusion (besides radiation). During September the shortcomings of the no-wind-mixing version become visible. During a sequence of warm days (i.e., net heat input at the surface), stable profiles tend to develop (as predicted by the no-wind-mixing version), but are eroded by wind-induced mixing.

The earlier wind-mixing algorithm in which $\frac{\Delta E_{pot}}{\Delta E_{kin}} = 1$ (Hurley Octavio et al., 1977) overpredicts mixing from the beginning. This effect accumulates during the summer, resulting in an overprediction of the thermocline depth of about 5 m in October. A slight overprediction of the new algorithm can also be observed during October, which could be attributed to the uncertainty of the constants used in the formulation of the algorithm, and to the limited wind fetch due to the small size of the lake.

4.2 Lake Anna, 1974

Lake Anna, a large lake shown in Figure 4-3, is formed by a dam on the North Anna River. The lake is located in central Virginia, 66 km northwest of Richmond. It has a surface area of 38.9 km^2 (at a design level of 75 m above sea level) and a volume of 3.0×10^6 m^3. The maximum depth at the dam is 21 m. The lake receives an average inflow of 7.7 m^3/s. Previous calculations have shown that throughflows can be neglected without changing the predicted profiles (Hurley Octavio et al., 1977).

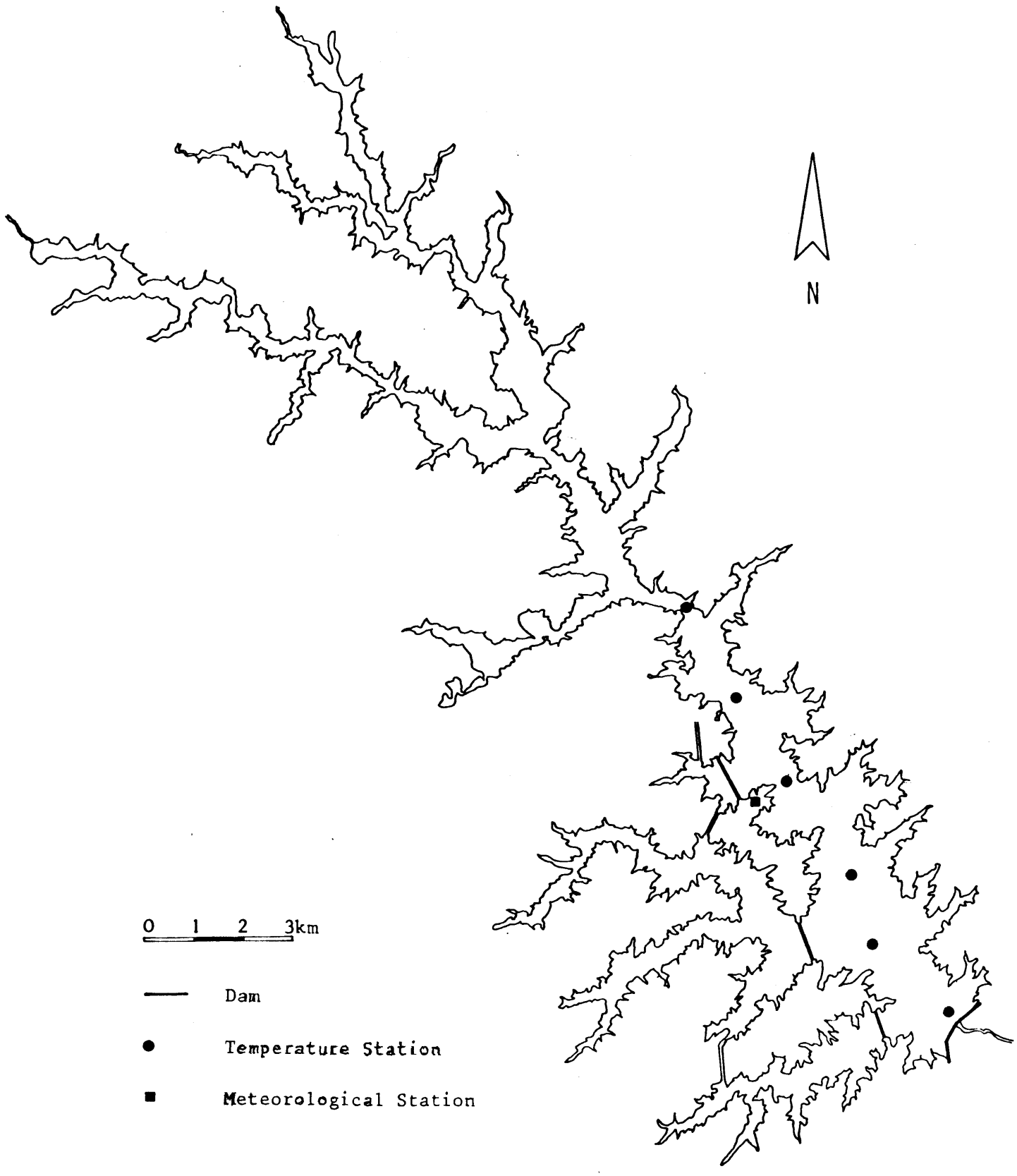

Fig. 4-3 Map of Lake Anna, Virginia

Intensive temperature surveys were conducted during 1974 in one to two months intervals. Profiles taken at six different locations (shown in Figure 4-3) were used for comparison. The measurements show some scatter up to three degrees centigrade near the thermocline, indicating the presence of seiches. In general, however, the measured temperature structure can be considered as one-dimensional. Meteorological data were obtained from a station near the lake, the measurement height was 15 m. The extinction coefficient $\eta = 0.5\ m^{-1}$, was determined from Secchi disk measurements and a value of $\beta = 0.5$ (Eq. 1-3a) was used. The calculations were started on April 6, 1974, when the lake was well-mixed at 11°C. An element thickness of 0.5 m and a time step of 1 day were chosen.

Again, the application of new wind-mixing algorithm provides the best agreement between measurements and predictions (Figure 4-4). The no-wind-mixing version is clearly not capable of simulating the various mixing events that are responsible for the rather complex temperature structure exhibiting two and more thermoclines during the summer. The overprediction of the earlier wind-mixing subroutine is significantly smaller as compared to Lake 226 NE (apart from the prediction of total mixing of the lake sometime in April, that did not take place). The temperature gradient in the thermocline region is smaller in Lake Anna than it is in Lake 226 NE. As a consequence, the density difference between two elements, and hence the local Richardson number have smaller values; thus dissipation plays only a minor role and the conversion process of kinetic to potential energy (i.e., entrainment) is still efficient.

4.3 Schoharie Reservoir, 1976

Schoharie Reservoir is located in the Catskill Mountains in upstate New York, approximately 64 km southwest of Albany (Figure 4-5). It is formed by a masonry dam across the valley of the Schoharie Creek at the north end

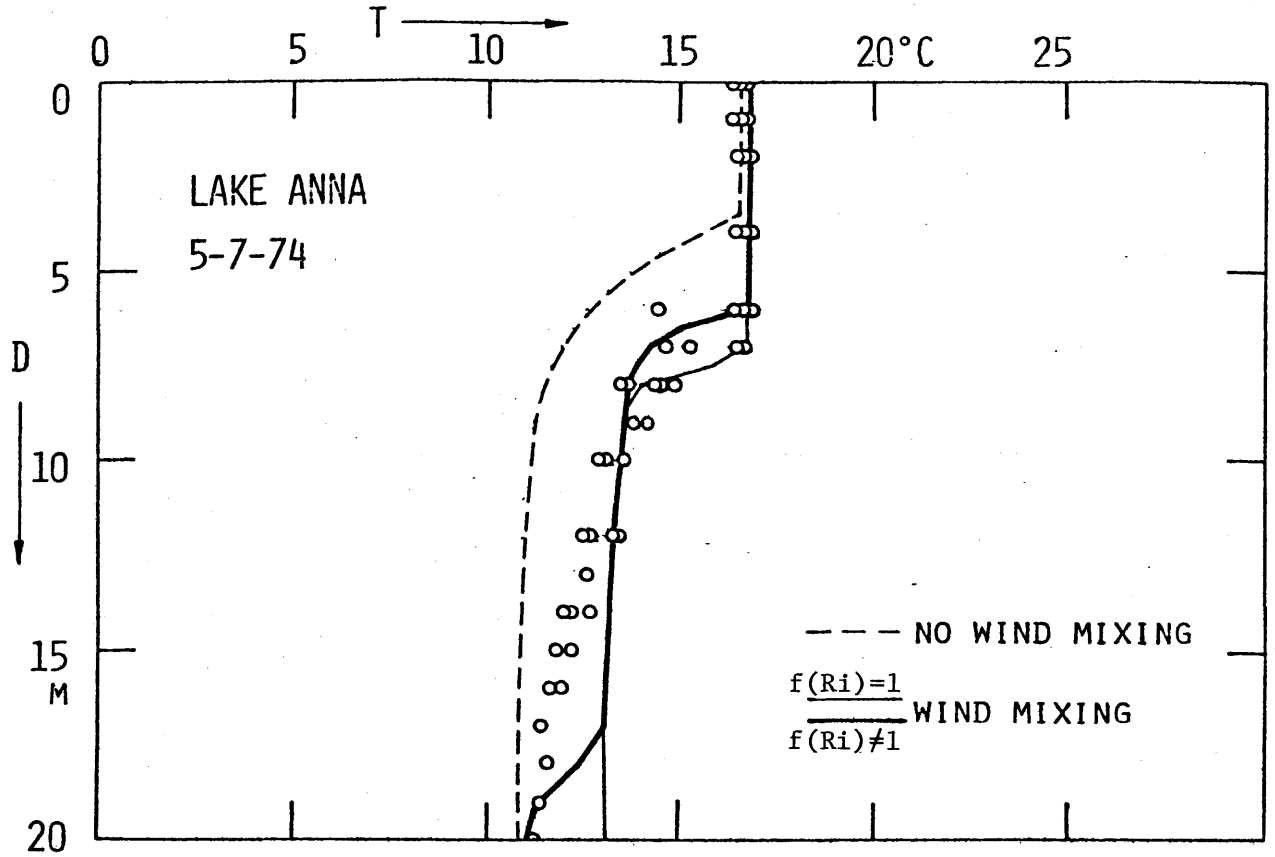

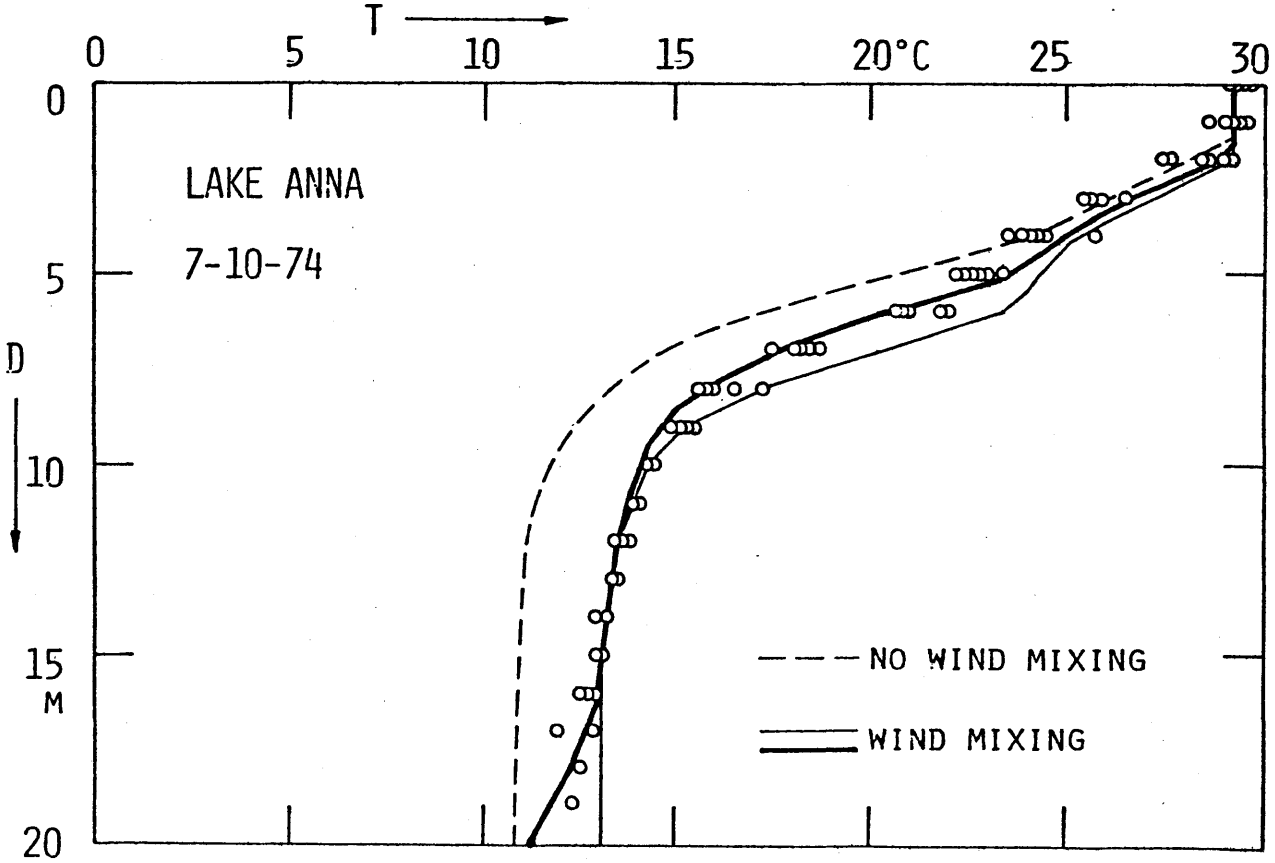

Fig. 4-4 Temperature Predictions for Lake Anna, Virginia

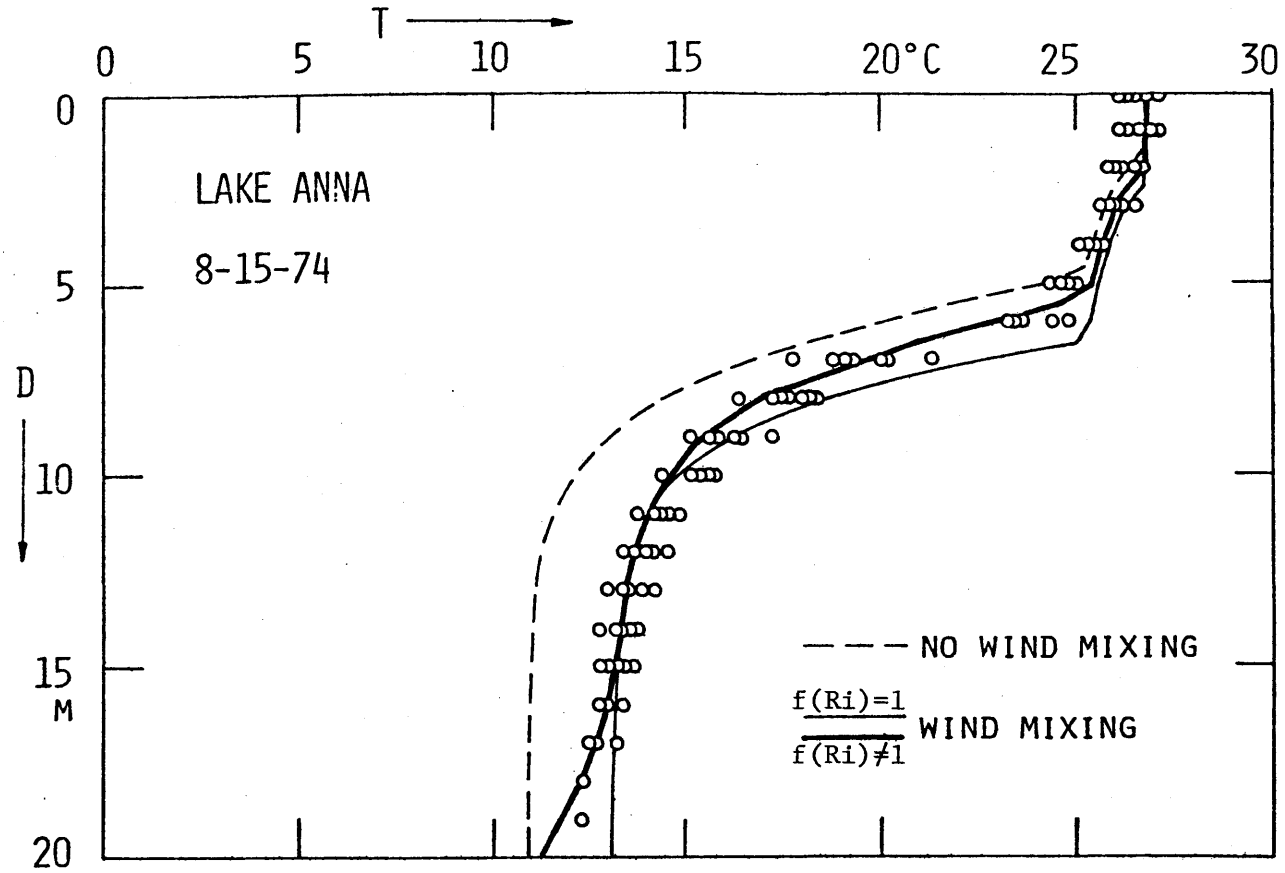

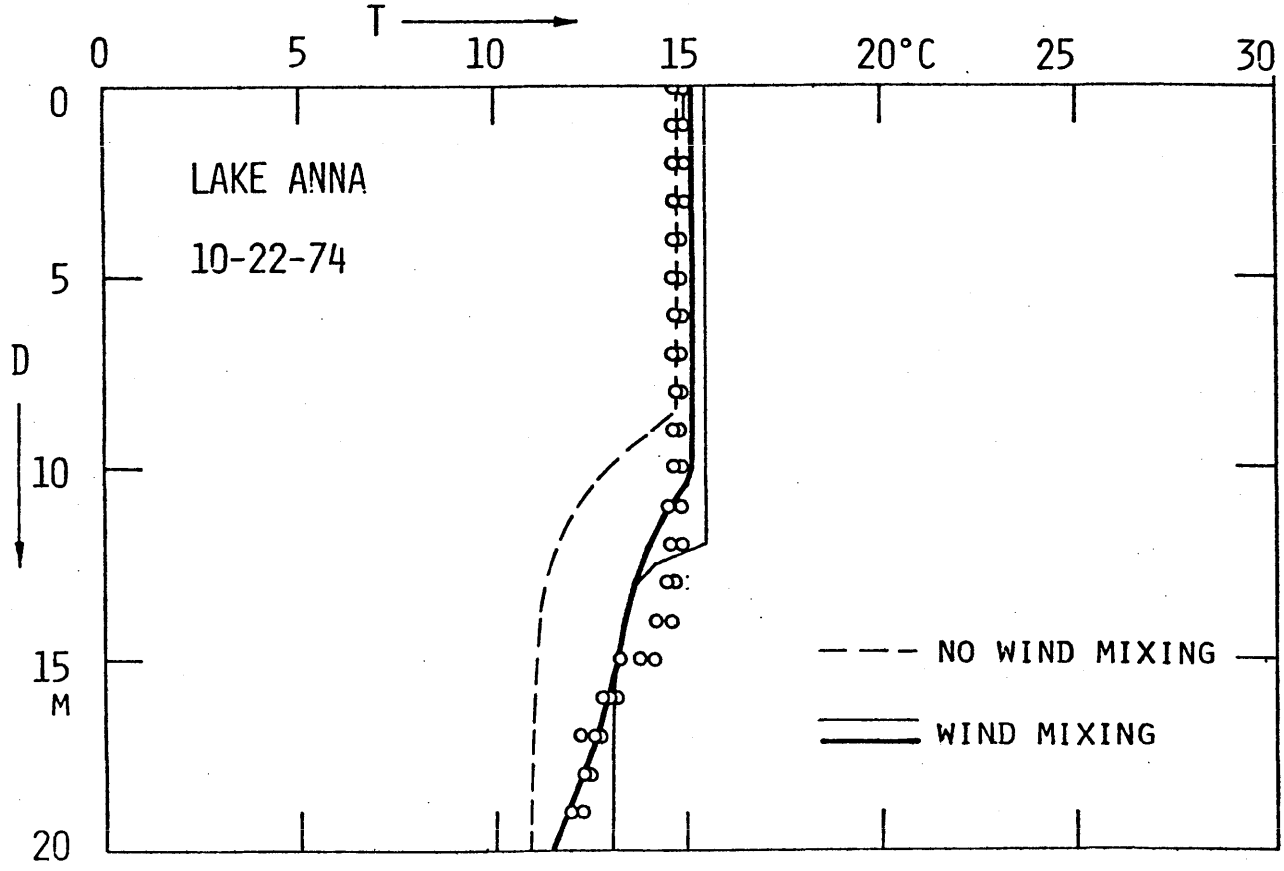

Fig. 4-4 (Continued)

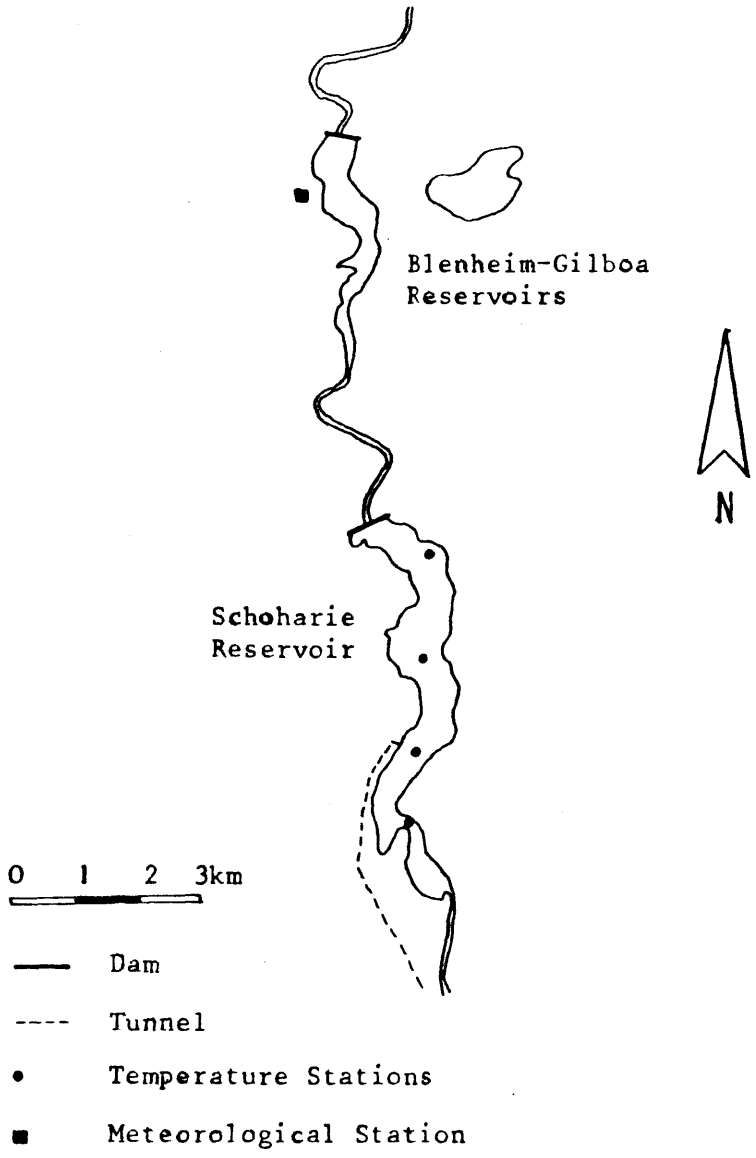

Fig. 4-5 Map of Schoharie Reservoir, New York

of the reservoir. At the crest elevation of the dam, 344 km above sea level, the surface area is 4.6 km^2, the length is about 9 km and the maximum width is about 1.1 km. The storage capacity at full pool is about 7×10^7 m^3 and the maximum depth at the dam is about 45 m. Inflows from Schoharie Creek at the south end of the reservoir and other tributaries average about 15 m^3/s. Outflows occur over the dam (primarily during winter) and through a tunnel (from late spring to early fall) which is utilized as part of the New York City water supply. The low level tunnel intake is located at the western shore of the reservoir at an elevation of 324 m, i.e., 20 m below maximum water level. The maximum flow rate through the tunnel in 1976 was 28.5 m^3/s.

Since local meteorological data (measured at the Blenheim-Gilboa Visitors' Center, several miles downstream) were available only for short periods of time, daily data from Albany Airport were used. The data was either used directly (in the case of cloud cover) or was linearly correlated with available measurements at the local station (in the case of air temperature and humidity). Because neither airport nor local wind speed data were representative of winds near the reservoir surface, a wind speed correction (equal to 45% of the wind speed at Albany) was obtained by comparing measured and predicted surface temperatures. Temperature profiles were measured once a week at locations indicated in Figure 4-5. The extinction coefficient $\eta = 0.5$ m^{-1} was determined from Secchi disk measurements and a value of $\beta = 0.5$ was chosen. Calculations were started on April 1, 1976 at a well-mixed temperature of 5°C. An element thickness of 2.0 m and a time step of 1 day were used.

Due to the relatively high throughflows (residence time of 55 days as compared to 450 days in Lake Anna) and due to the submerged outlet it

can be expected that throughflows dominate the seasonal temperature development and that vertical diffusion and wind-mixing are of less importance. Hurley Octavio, et al. (1977) have derived a dimensionless number similar to a Péclet number, that relates the effects of vertical diffusion and advection: $Pe = \frac{Qz_o}{AE}$. Q is the flow rate through the outlet at a depth z_o, A is the cross-sectional area at that depth, and E is the vertical diffusivity.

If Pe >> 1, advection dominates diffusion. With E equal to molecular diffusion, Pe $\sim 3 \times 10^3$ for Schoharie Reservoir. A larger eddy diffusivity would still yield Pe >> 1. An advection dominated temperature structure can, therefore, be expected.

Predicted and measured profiles are plotted in Figures 4-6. Since the surface elevation changes considerably during the year, the elevation above sea level was chosen as ordinate. The predictions of the three versions of the model are all within the scatter of the measured data and are very similar, which is consistent with the criteria given above. (Similar insensitivity to turbulent vertical mixing has been found in Fontana Reservoir, North Carolina, by Huber and Harleman (1968)). Some small differences between the no-wind-mixing and the wind-mixing versions are found in the surface layer when wind-mixing erodes stable but weak gradients which would otherwise form in April and May (due to net heat input) and in November (due to heat loss, after the reservoir has passed through the density maximum). It is noteworthy that the subcooling of the surface, as predicted by the no-wind-mixing version for November 15, 1976, was supported by measurements taken in the upper part of the reservoir which was evidently sheltered against the prevailing winds on that day.

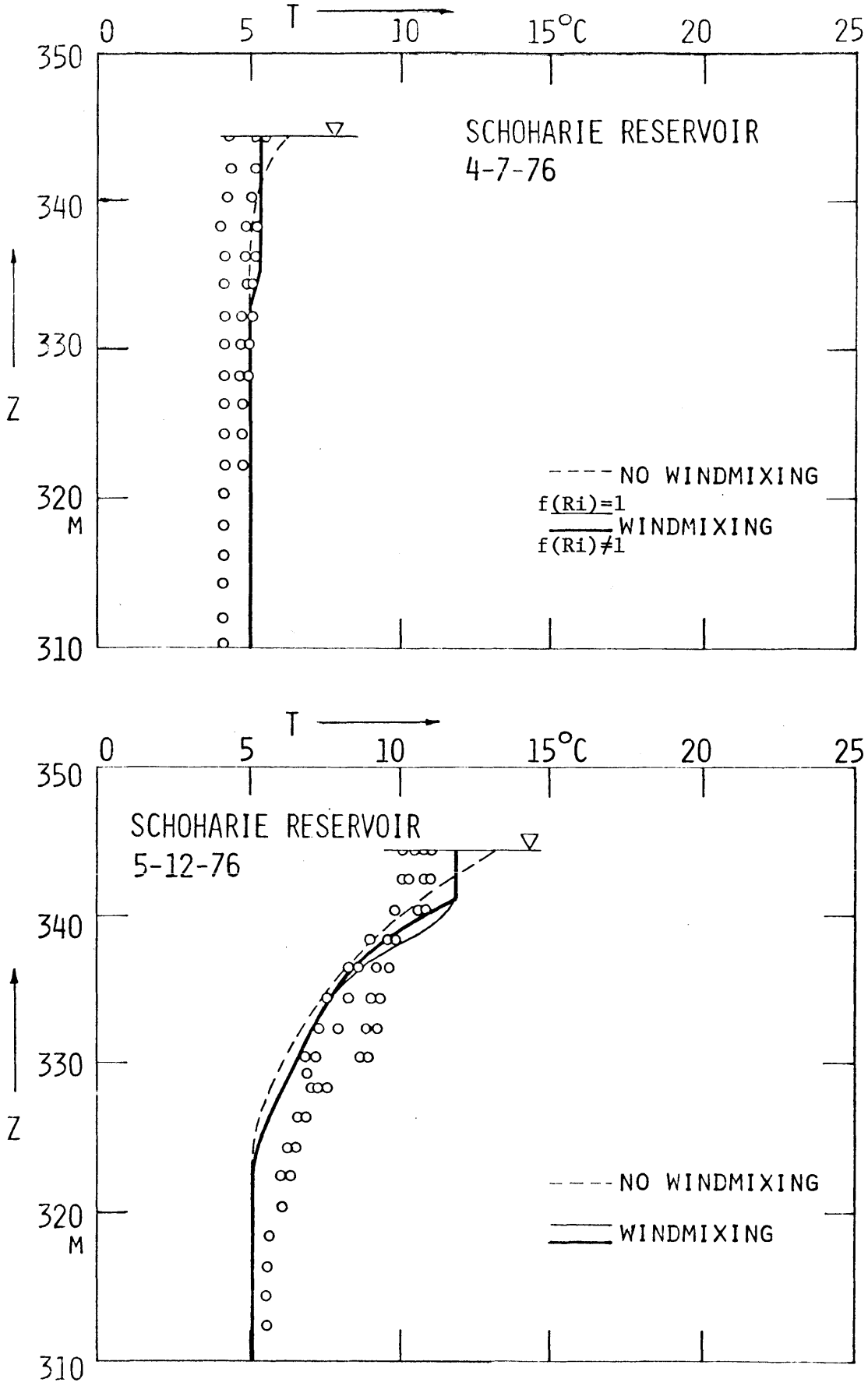

Fig. 4-6 Temperature Predictions for Schoharie Reservoir, New York (Continued)

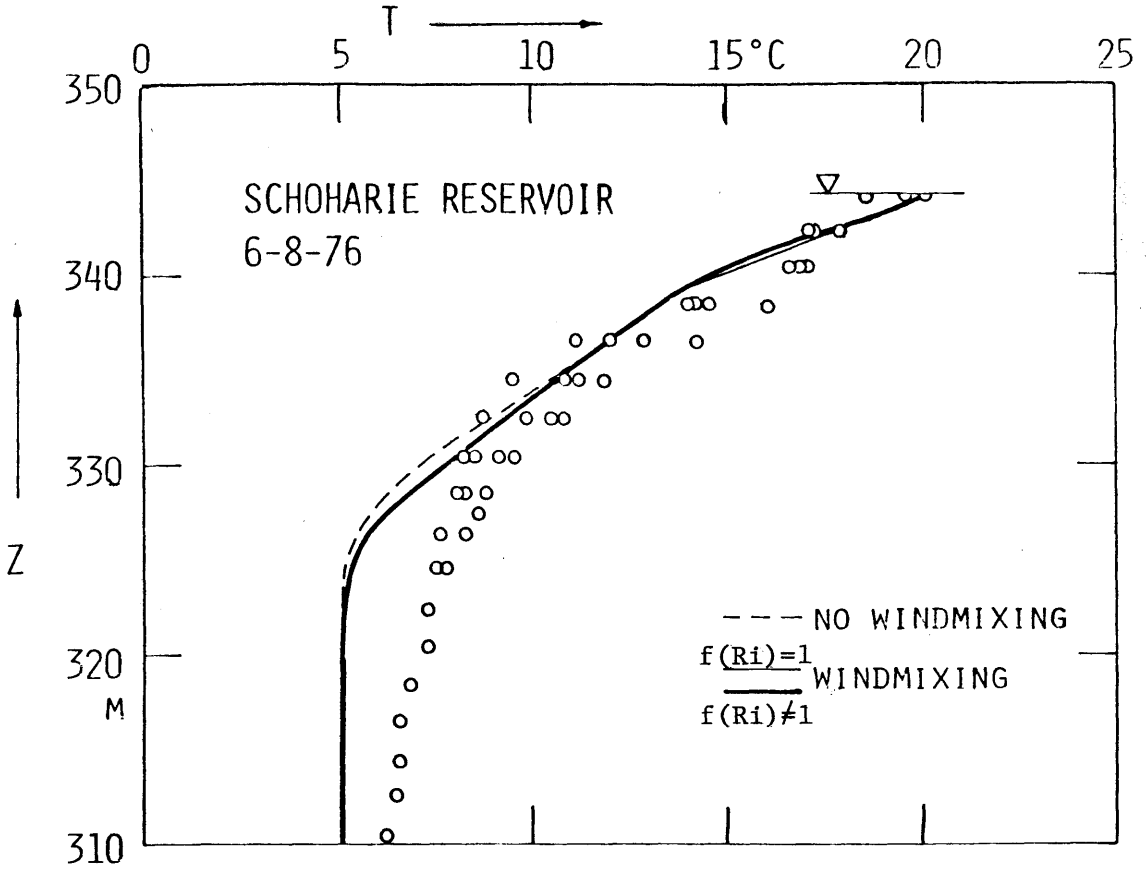

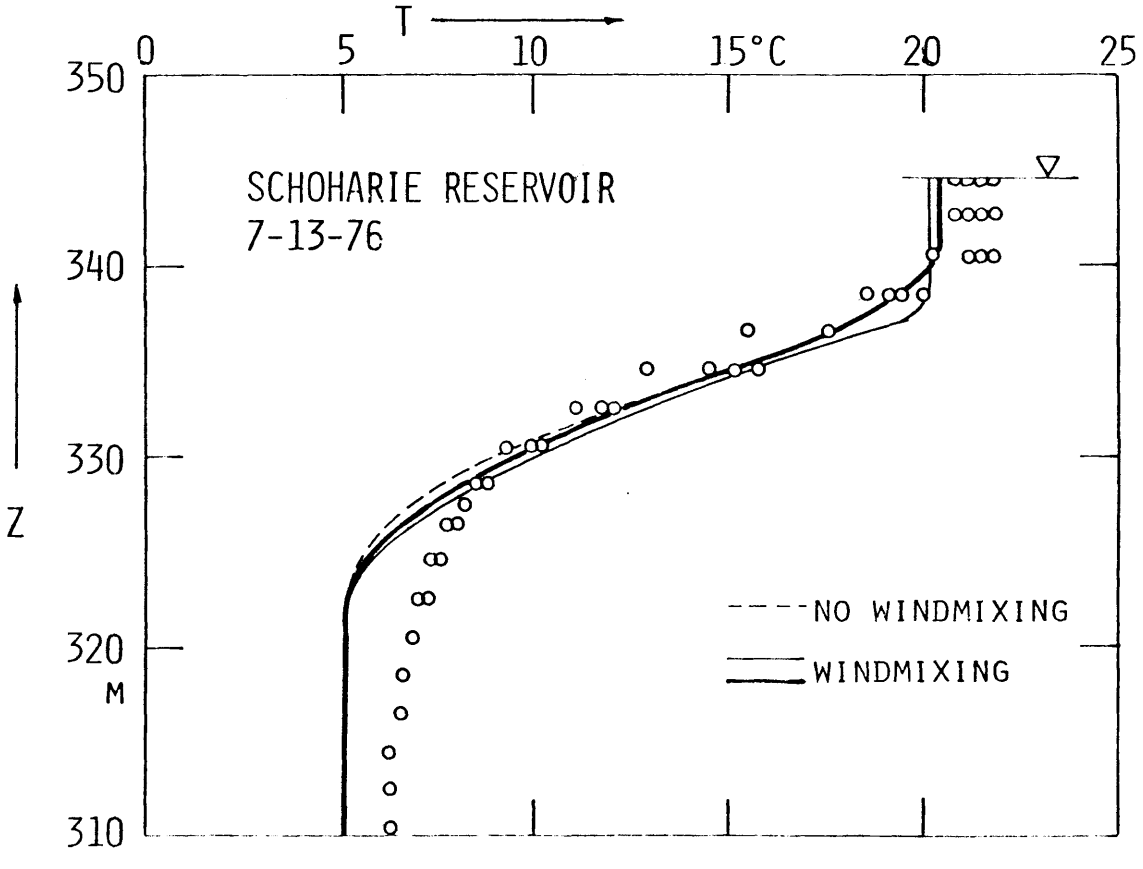

Fig. 4-6 (Continued)

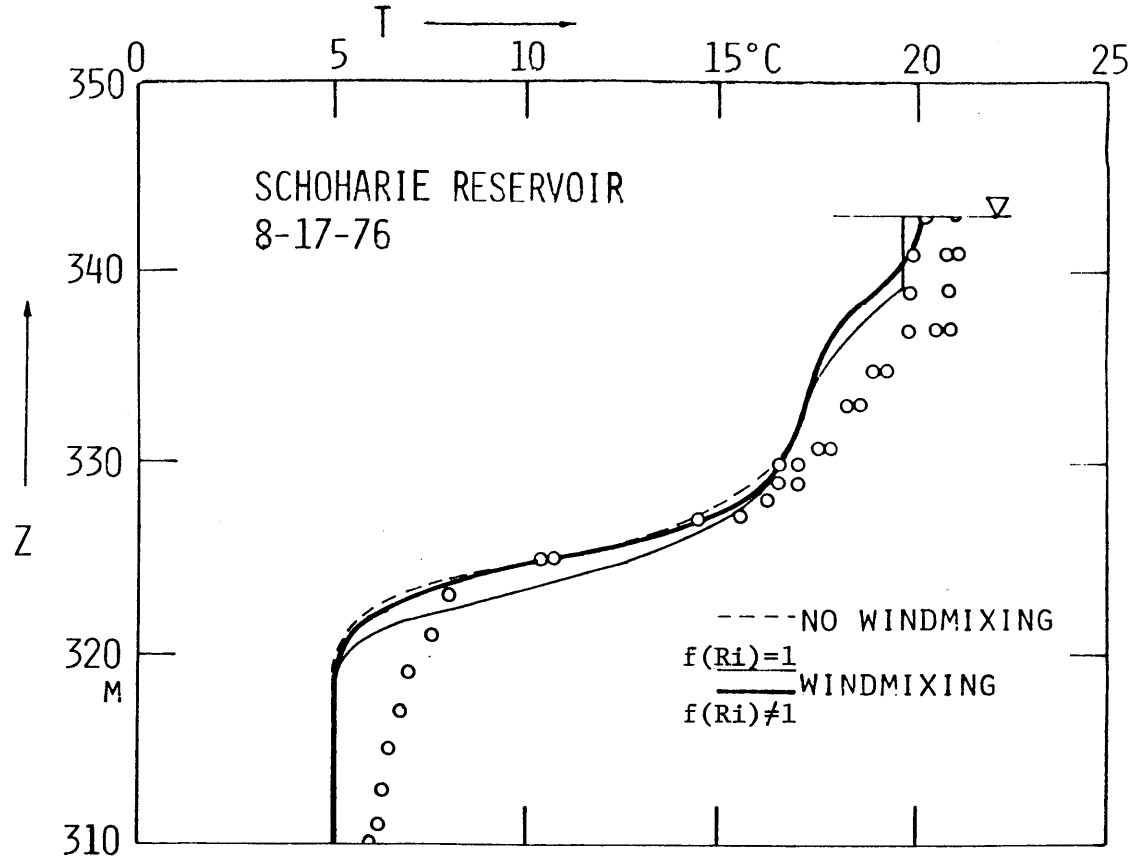

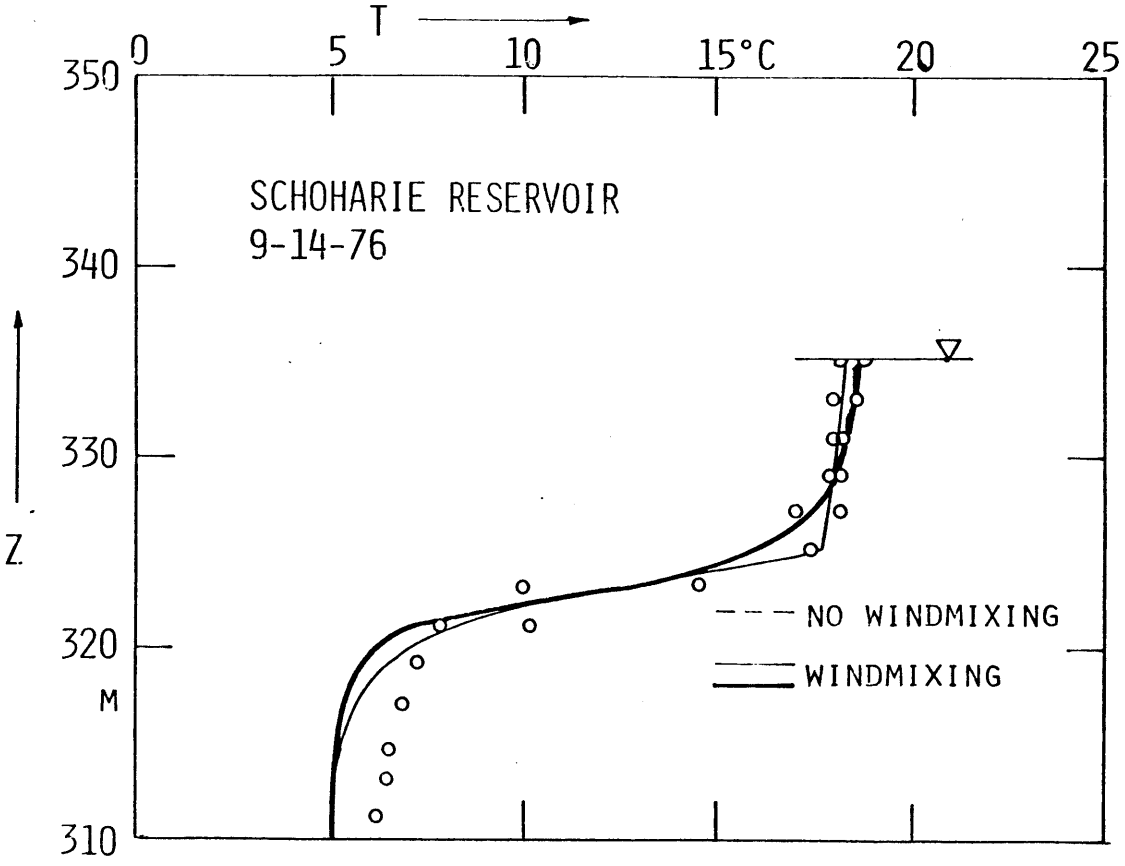

Fig. 4-6 (Continued)

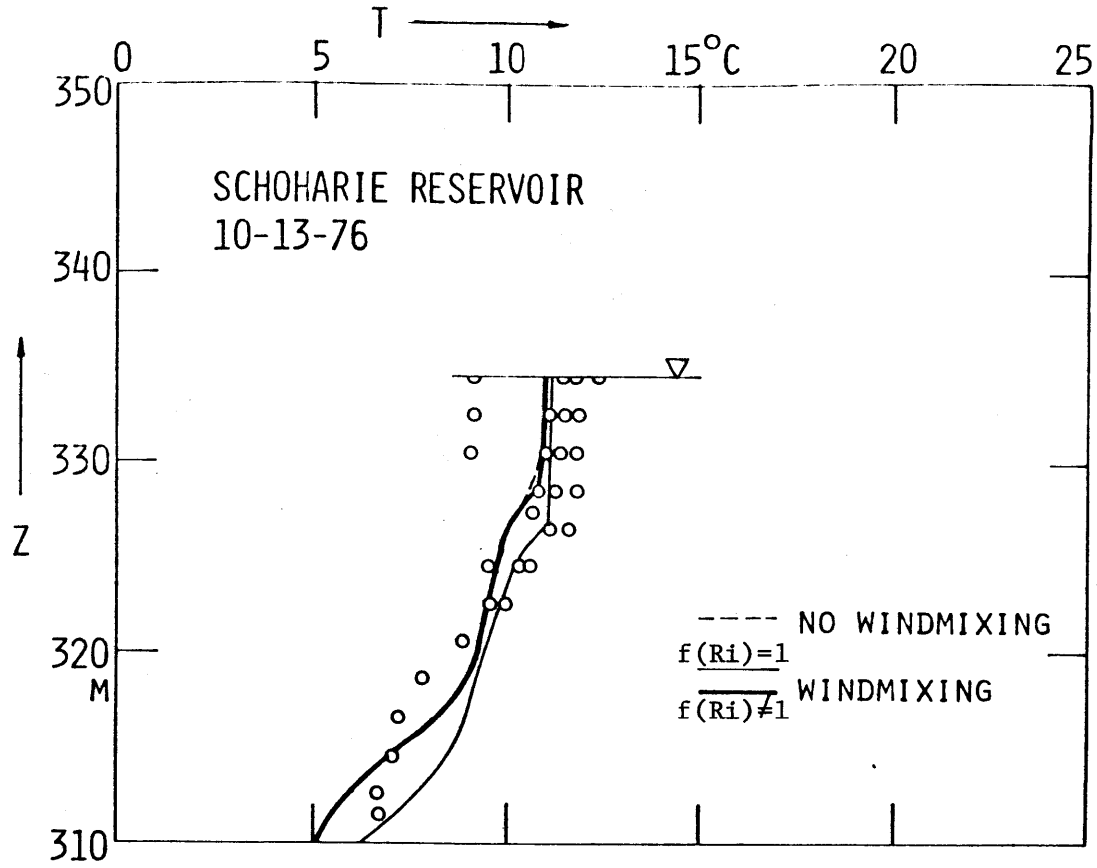

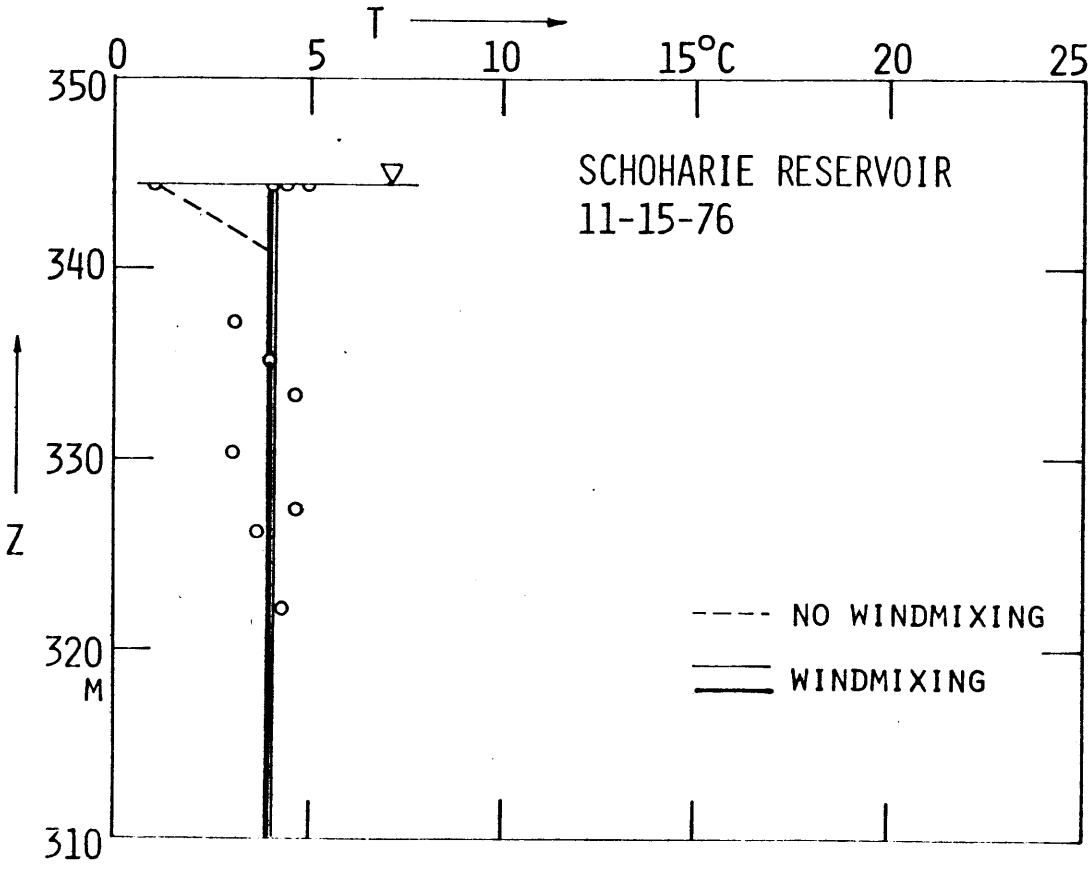

Fig. 4-6 (Continued)

V. Sensitivity of the MIT Lake and Reservoir Model

5.1 Element Thickness and Time Step

Previous sensitivity studies (Hurley Octavio et al. (1977)) have shown that predicted profiles are not sensitive to the element thickness for element sizes in the range 0.5m to 2m (except for additional resolution at the top of the thermocline for the smaller elements). Since the density difference between two elements and hence the Richardson number criterion depend on the distance between two elements in the new subroutine, grid spacings of 0.5 m and 1 m were tested and the results were essentially identical. For reservoirs with high through-flows, where the temperature development is dominated by advection, an element thickness of 2m will yield good results.

Intervals between 1/8 of a day and one day were used to study the sensitivity with respect to the time step. Almost identical results were obtained for the summer stratification period, but a slight underprediction of mixing in early spring could be detected for smaller time steps. This can be explained as follows: during the fully developed stratification period, the density difference between two elements is determined by the local gradient while effects of daily heating are negligible; but for the very weak stratification in spring, the change of the density difference between two elements due to daily heating may be of the same order as the difference itself. Subdivision of the time step, therefore, decreases the Richardson number and, hence, limits entrainment due to transient effects.

In general, an element thickness between 0.5m and 1m and a time step of 1 day is recommended.

5.2 Vertical Diffusivity

Lake Anna data for 1974 were used to examine the performance of the MIT model when turbulent trnasport is modeled by an increase eddy diffusivity rather than by a wind-mixing algorithm. Results for molecular, 10 times molecular and 50 times molecular diffusivity (but without wind-mixing) were compared to the results for the new wind-mixing algorithm (as the best representation of the measurements) in Figure 5-1. Although the predicted profiles for an eddy diffusivity of 10x molecular are comparatively similar to the standard profiles, they do not show the fine-structure of the measured profiles reflecting the time history of alternate heating, cooling and wind-mixing events. In general, eddy diffusivity models cannot predict the details of the seasonal temperature development, unless they use a time-varying, depth-dependent turbulent diffusion coefficient.

5.3 Extinction Coefficient

Measurements of the extinction coefficient are usually not readily available. Secchi disk measurements allow only a rough estimate of its value. The sensitivity of the MIT model, including the new wind-mixing algorithm, to the magnitude of the extinction coefficient has, therefore, been examined using Lake Anna data from 1974. The results are given in Figure 5-2. They show that an increase of the coefficient from 0.25 m^{-1} (clear) to 1 m^{-1} (turbid) results in a considerable upward ship of the thermocline. (A value of 0.5 m^{-1} was chosen for the standard run.) This effect emphasizes the necessity of accurate measurements of extinction coefficients, if a temperature prediction model is to be applied without "calibration" parameters.

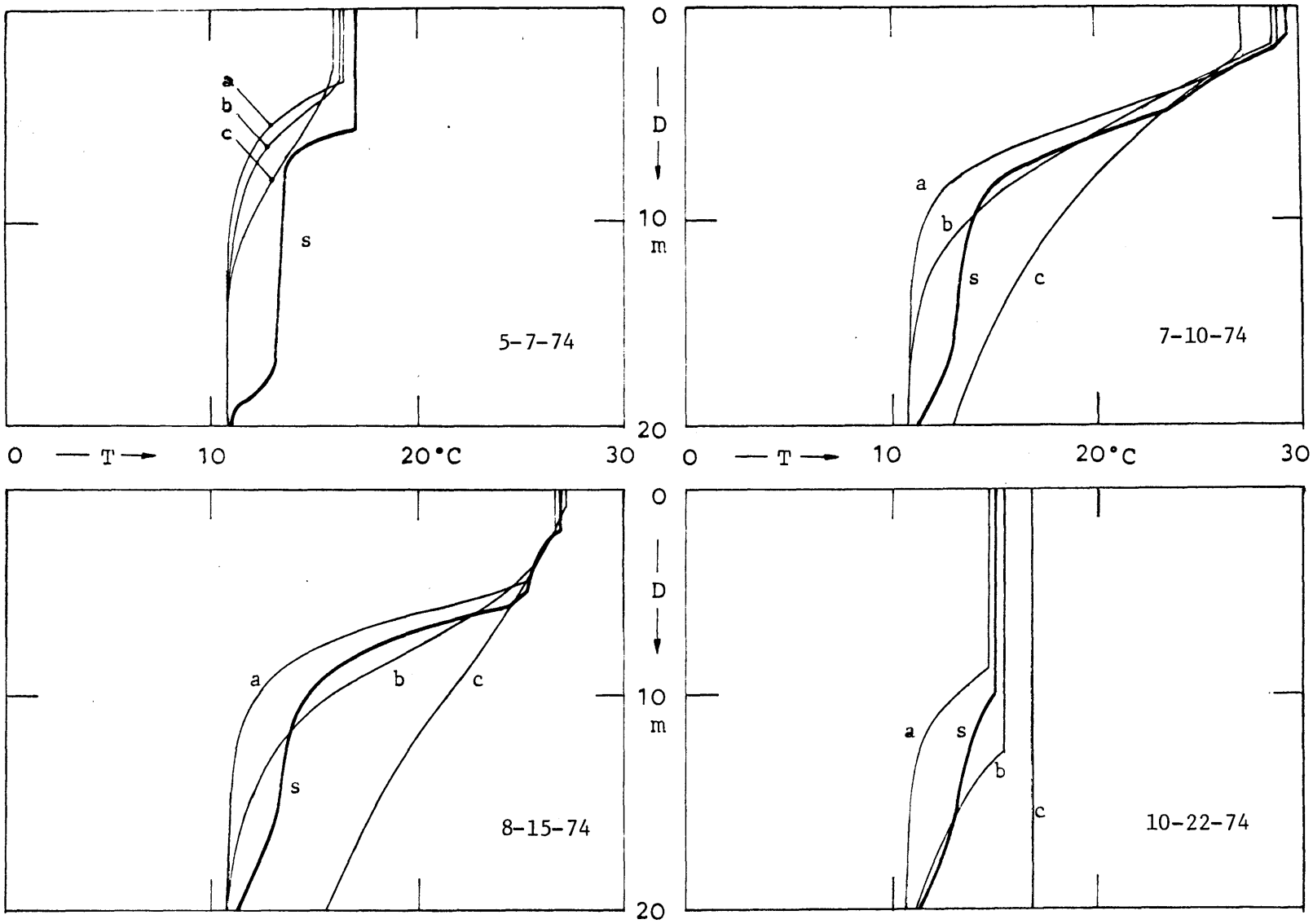

Fig. 5-1 Effect of Vertical Diffusivity a: Molecular Diffusivity, b: 10 x Molecular, c: 50 x Molecular, s: Standard Run Using new Wind Mixing Algorithm.

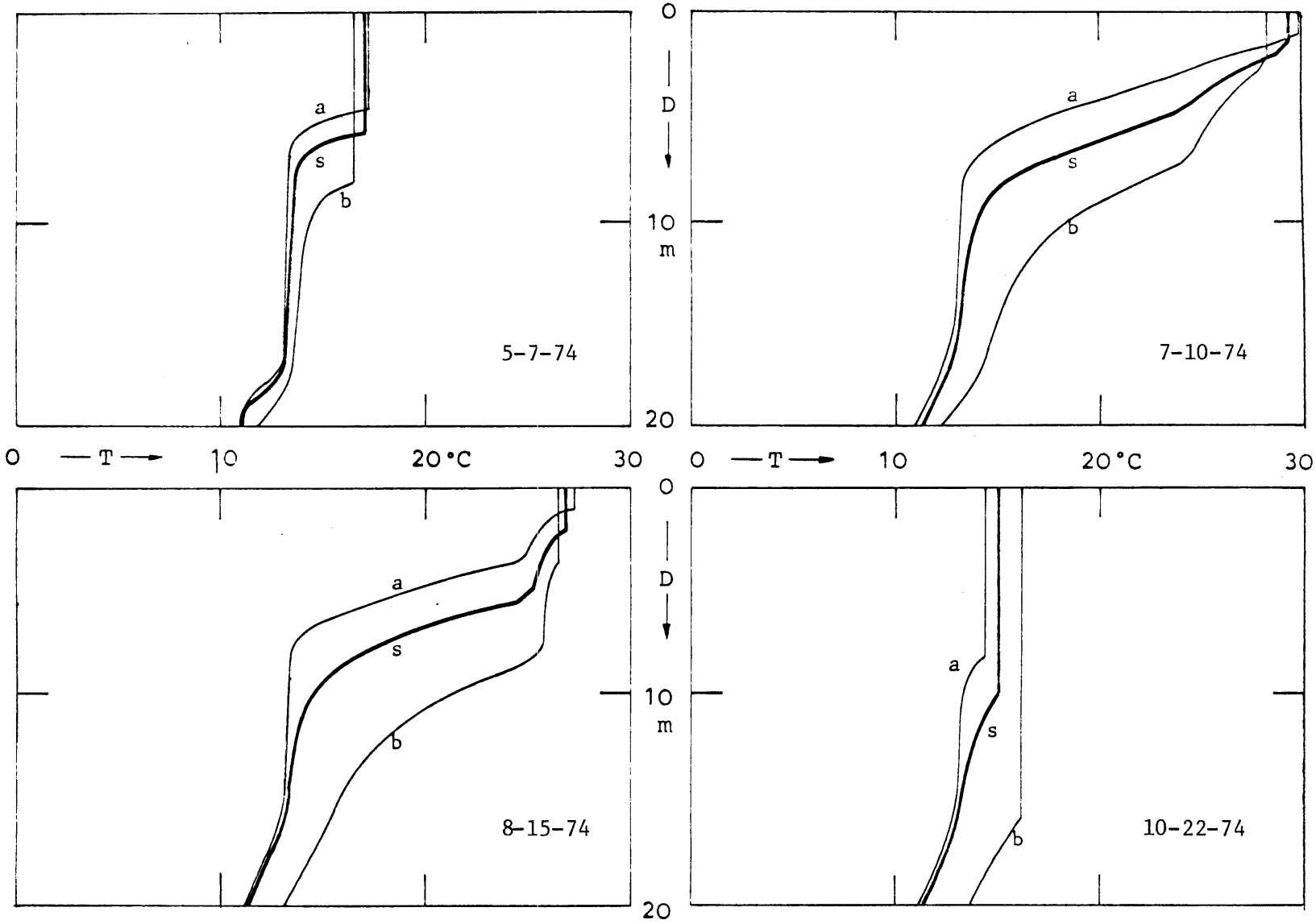

Fig. 5-2 Effect of Extinction Coefficient on new Wind Mixing Algorithm
(a: $\eta = 1\ m^{-1}$, s: $\eta = 0.5\ m^{-1}$ (Standard Run), c: $\eta = 0.25\ m^{-1}$)

5.4 Effect of Shear Stress at the Thermocline

Temperature measurements of Lake Anna have indicated the presence of internal seiches. Currents associated with the seiching motions can produce shear stress at the thermocline, so that the situation may be better represented by the application of a wind-mixing algorithm according to eq. (3-16b), where shear stress production balances dissipation, than by eq. (3-16a) that was used in Chapter 4.2. The results showed that both algorithms predicted the limited mixing in spring correctly, but that eq. (3-16b) overpredicts wind-mixing in the same way as the earlier wind-mixing algorithm throughout summer and fall. This fact not only proves that shear stress does not balance dissipation in this case but also allows an interesting conclusion. For low Richardson numbers, eq. (3-16a) shows the same behavior as eq. (3-16b), while for higher Richardson numbers eq. (3-16b) approaches the Ri^{-1} law, i.e. the earlier wind-mixing subroutine without dissipation effects. That means that in spring, the entrainment process is limited by transient effects, while during summer and fall it is less efficient due to dissipation.

VI Summary and Conclusions

A new wind-mixing algorithm has been developed that accounts for transient and dissipation effects on the conversion of TKE into potential energy during the entrainment process. The new version of the MIT Lake and Reservoir Model has been applied to two lakes of different size, and to a reservoir, with good results. It should be mentioned that in the case of Lake 226 NE, all input data (including the absorption coefficient) were measured so that no calibration or fitting parameters were used in the runs.

The results that were presented in Chapter 4 seem to indicate the existence of "self-preserving" behavior of the thermocline. Once a strong stratification has formed later in spring (due to high extinction coefficients, strong insolation or low winds), this stable gradient causes a high dissipation rate of the wind-induced turbulence, and will not be eroded until fall, when surface cooling begins to predominate. On the other hand, when only a weak gradient forms during spring, a very efficient entrainment process "gnaws" at the thermocline throughout the summer and prevents the later development of a stabler thermocline. By comparing different versions of the wind-mixing algorithm with measurements, the thermocline depth overprediction of the earlier wind-mixing subroutine has been explained. During spring, entrainment is reduced because part of the energy input is used to increase the content of TKE of the rapidly growing mixed layer. The overprediction in fall resulted from the accumulative effect of the neglect of dissipation during the summer stratification.

Sensitivity studies with respect to eddy diffusivity and extinction coefficient have shown that reasonable agreement between measurements and predictions can be achieved also with less sophisticated models by using these parameters for fitting the measured profiles. The quality of

a temperature prediction model should, therefore, not be judged by a fair overall agreement in one case of application but by the ability to describe the seasonal temperature development in detail, locally and with time, for different sites without the use of fitting parameters.

Further improvements of the presented model can be made with respect to kinetic energy transfer across the air-water interface. The fact that the same model slightly overpredicts mixing in October for the small Lake 226 NE, but underpredicts it for the larger Lake Anna, suggests a dependence of the energy transfer on the fetch; however, the airflow above the lake surface is not only affected by the lake size and shape but also by the topology and vegetation of the environment. Information about these factors is not always easily available. In Chapter 3.3, it was mentioned that the surface shear stress coefficient C_Z is a function of the stability of the ambient air. Modelling this effect requires detailed knowledge of the temperature distribution in the air above the lake. Again, this information is usually not available.

REFERENCES

Ball, F.K., "Control of Inversion Height by Surface Heating", Quart.J. Roy. Met. Soc. 86, pp 483-494, 1960.

Barnum, D.C. and Rao, G.V., "Role of Advection and Penetrative Convection in Affecting the Mixing-Height Variations over an Idealized Metropolitan Area", Bound. Layer Meteor. 8, pp 497-514, 1975.

Batchelor, G.K., "The Theory of Homogeneous Turbulence", Cambridge University Press, 1953.

Betts, A.K., "Non-Precipitating Cumulus Convection and its Parameterization", Quart. J. Roy. Met. Soc. 99, pp 178-196, 1973.

Busch, N.E., "Fluxes in the Surface Boundary Layer Over the Sea", Chapter 6, pp 72 - 91, Modelling and Prediction of the Upper Layers of the Ocean, Edited by E.B. Kraus, Pergamon Press, 1977

Charnock, H., "Wind-Stress on a Water Surface", Quart. J. Roy. Met. Soc. 81, pp 639, 1955.

Carson, D.J., "The Development of a Dry Inversion-Capped Convectively Unstable Boundary Layer", Quart. J. Roy. Met. Soc. 99, pp 450-467, 1973.

Cattle, H. and Weston, K.J., "Budget Studies of Heat Flux Profiles in the Convective Boundary Layer Over Land", Quart. J. Roy. Met. Soc. 101, pp. 353-363, 1975.

Coantic, M.F., "Coupled Energy Transfer and Transformation Mechanisms Across the Ocean-Atmosphere Interface", Proc. 6th Int. Heat Transfer Conf., Vol. 6, Toronto, Canada, 1978.

Deardorff, J.W., "Convective Velocity and Temperature Scales for the Unstable Planetary Boundary Layer and for Rayleigh Convection", J. Atmos. Sci. 27, pp 1211-1213, 1970.

Deardorff, J.W., "Three-Dimensional Numerical Study of the Height and Mean Structure of a Heated Planetary Boundary Layer", Bound. Layer Meteor. 7, pp 81-106, 1974.

Deardorff, J.W., Willis, G.E. and Lilly, D.K., "Comment on the Paper by A.K. Betts, 'Non-Precipitating Cumulus Convection and its Parameterization'", Quart. J. Roy. Met. Soc. 100, pp 122-123, 1974.

Denman, K.L., "A Time-Dependent Model of the Upper Ocean", J. Phys. Oceanogr. 3, pp 173-184, 1973.

Denton, R.A., "Entrainment by Pénetrative Convection at Low Peclet Number", Research Report, Department of Civil Engineering, University of Canterbury, Christchurch, New Zealand, January 1978.

Denton, R.A. and Wood, I.R., "Convective Motions and Resulting Entrainment in a Two-Layered Fluid System Heated from Below", Proc. 5th Australasian Conf. on Hydraulics and Fluid Mech., Vol. II, pp 361-368, 1974.

Hasselmann, K, et XV al, "Measurements of Wind Wave Growth and Swell Decay During the Joint North Sea Wave Project (JONSWAP)", Deutsch. Hydrograph. Institut, Reich A, No. 12, 1973.

Heidt, F.D., "Zeitlicher Abbau der Stabilen Schichtung eines Fluids durch freie Konvektion", Diss. Universität Karlsruhe, B.R.D., 1975.

Hopfinger, E.J. and Toly, J. A., "Spatially Decaying Turbulence and its Relation to Mixing Across Density Interfaces", J. Fluid Mech. 78, pp 155-175, 1976.

Huber, W.C. and Harleman, D.R.F., "Laboratory and Analytical Studies of Thermal Stratification in Reservoirs", R.M. Parsons Laboratory Technical Report No. 112, Massachusetts Institute of Technology, 1968.

Hurley Octavio, K.H., Jirka, G.H. and Harleman, D.R.F., "Vertical Heat Transport Mechanisms in Lakes and Reservoirs", R.M. Parsons Laboratory Technical Report No. 227, Massachusetts Institute of Technology, 1977.

Jenkins, B.S., "Studies of the Flow of a Fluid with Density Differences Caused by Turbidity", Water Res. Lab., Report No. 133, University of New South Wales, 1973.

Kantha, L.H., Phillips, O.M. and Azad, R.S., "On Turbulent Entrainment at a Stable Density Interface", J. Fluid Mech. 79, pp 753-768, 1977.

Kato, H. and Phillips, O.M., "On the Penetration of a Turbulent Layer into a Stratified Fluid", J. Fluid Mech. 37, pp 643-655, 1969.

Kondo, J., Sasano, Y. and Ishii, T., "On Wind-Driven Current and Temperature Profiles with Diurnal Period in the Oceanic Planetary Boundary Layer", J. Phys. Oceanogr. 9, pp 360-372, 1979.

Kraus, E.B. and Turner, J.S., "A One-Dimensional Model of the Seasonal Thermocline", Tellus 19, pp 98-106, 1967.

Lilly, D.K., "Models of Cloud-Topped Mixed Layers under a Strong Inversion" Quart. J. Roy. Met. Soc. 94, pp 292-309, 1968.

Linden, P.F., "The Interaction of a Vortex Ring with a Sharp Density Interface: A Model for Turbulent Entrainment", J. Fluid Mech. 60, pp 467-480, 1973.

Linden, P.F., "The Deepening of a Mixed Layer in a Stratified Fluid", J. Fluid Mech. 71, pp 385-405, 1975.

Madsen, O.S., "A Realistic Model of the Wind-Induced Ekman Boundary Layer", J. Phys. Oceanogr. 7, pp 248-255, 1977.

Moore, M.J. and Long, R.R., "An Experimental Investigation of Turbulent Stratified Shearing Flow", J. Fluid Mech. 49, pp 635-655, 1971.

Munk, W.H. and Anderson, E.R., "Notes on a Theory of the Thermocline", J. Marine Research 7, pp 276-295, 1948.

Orlob, G.T., "Mathematical Models for Prediction of Thermal Energy Changes in Impoundments", Final Report to FWQA by Water Res. Eng., Inc., 1969.

Pederson, F.B., "The Bulk Flux Richardson Number Applied on Turbulent Entrainment at a Stable Density Interface", Tech. Univ. Denmark, Inst. Hydrodyn. and Hydraulic Engg., Prog. Rep. No. 43, 1977.

Phillips, O.M., "The Dynamics of the Upper Ocean", Cambridge University Press, 1977.

Rayment, R. and Readings, C.J., "A Case Study of the Structure and Energetics of an Inversion", Quart. J. Roy. Met. Soc. 100, pp 221-233, 1974.

Readings, C.J., "Some Aspects of the Cardington Research Program", Quart. J. Roy. Met. Soc. 99, pp 764-767, 1973.

Rouse, H. and Dodu, J., "Diffusion Turbulente à Travers une Discontinuité de Densité", La Houille Blanche 10, pp 522-532, 1955.

Ryan, P.J. and Harleman, D.R.F., "Prediction of the Annual Cycle of Temperature Changes in a Stratified Lake or Reservoir: Mathematical Model and User's Manual", R.M. Parsons Laboratory Technical Report No. 137, Massachusetts Institute of Technology, 1971.

Sacharik, E.S., "The Tropical Mixed Layer and Cumulus Parameterization", J. Atmos. Sci. 31, pp 2225-2230, 1974.

Sherman, F.S., Imberger, J. and Corcos, G.M., "Turbulence and Mixing in Stably Stratified Waters", Ann. Rev. Fluid Mech. 10, pp 267-288, 1978.

Spalding, D.B. and Svensson, U., "The Development and Erosion of the Thermocline", Proc. 1976 Seminar of the Int. Centre for Heat and Mass Transfer, Belgrade, Yugoslavia , 1976.

Stefan, H. and Ford, D.E., "Temperature Dynamics in Dimictic Lakes, J. Hydraul. Div., ASCE 101, pp 97-114, 1975.

Stull, R.B., "Inversion Rise Model Based on a Penetrative Convection", J. Atmos. Sci. 30, pp 1092-1099, 1973.

Stull, R.B., "The Energetics of Entrainment Across a Density Interface", J. Atmos. Sci. 33, pp 1260-1267, 1976.

Sundaram, T.R. and Relm, R.G., "The Seasonal Thermal Structure of Deep Temperate Lakes", Tellus 25, pp 157-167, 1973.

Svensson, U., "A Mathematical Model of the Seasonal Thermocline", Thesis Report No. 1002, Department of Water Res. Engr., Lund Institute of Technology, Lund, Sweden, 1978.

Sverdrup, H.U., "Oceanography for Meteorologists", George Allen and Unwin, Ltd., Lindon, 1945.

Tennekes, H., "A Model for the Dynamics of the Inversion Above a Convective Boundary Layer", J. Atmos. Sci. 30, pp 558-567, 1973.

Thompson, S. and Turner, J.S., "Mixing Across an Interface Due to Turbulence Generated by an Oscillating Grid", J. Fluid Mech. 67, pp 349-368, 1975.

Tucker, W.A. and Green, A.W., "A Time-Dependent Model of the Lake-Averaged, Vertical Temperature Distribution of Lakes", Limnol. Oceanogr. 22, pp 687-699, 1977.

Turner, J.S., "The Influence of Molecular Diffusivity on Turbulent Entrainment Across a Density Interface", J. Fluid Mech. 33, pp 639-656, 1968.

Turner, J.S., "Buoyancy Effects in Fluids", Cambridge University Press, 1973.

Willis, G.E. and Deardorff, J.W., A Laboratory Model of the Unstable Planetary Boundary Layer", J. Atmos. Sci. 31, pp 1297-1307, 1974.

Wolanski, E.J. and Brush, L.M., "Turbulent Entrainment Across Stable Density Step Structures", Tellus 27, pp 259-268, 1975.

Wu, J., "Wind-Induced Turbulent Entrainment Across a Stable Density Interface", J. Fluid Mech. 61, pp 275-287, 1973.

Wu, J., "An Alternative Analysis of Entrainment Data from a Circular Annular Tank under Constant Stress", College of Marine Studies, University of Delaware, September 1978.

Zeman, O. and Tennekes, H., "Parameterization of the Turbulent Energy Budget at the Top of the Daytime Atmospheric Boundary Layer", J. Atmos. Sci. 34, pp 111-123, 1977.

Zilitinkevich, S.S., "Comments on 'A Model for the Dynamics of the Inversion Above a Convection Boundary Layer'", J. Atmos. Sci. 32, pp 991-992, 1975.

LIST OF FIGURES